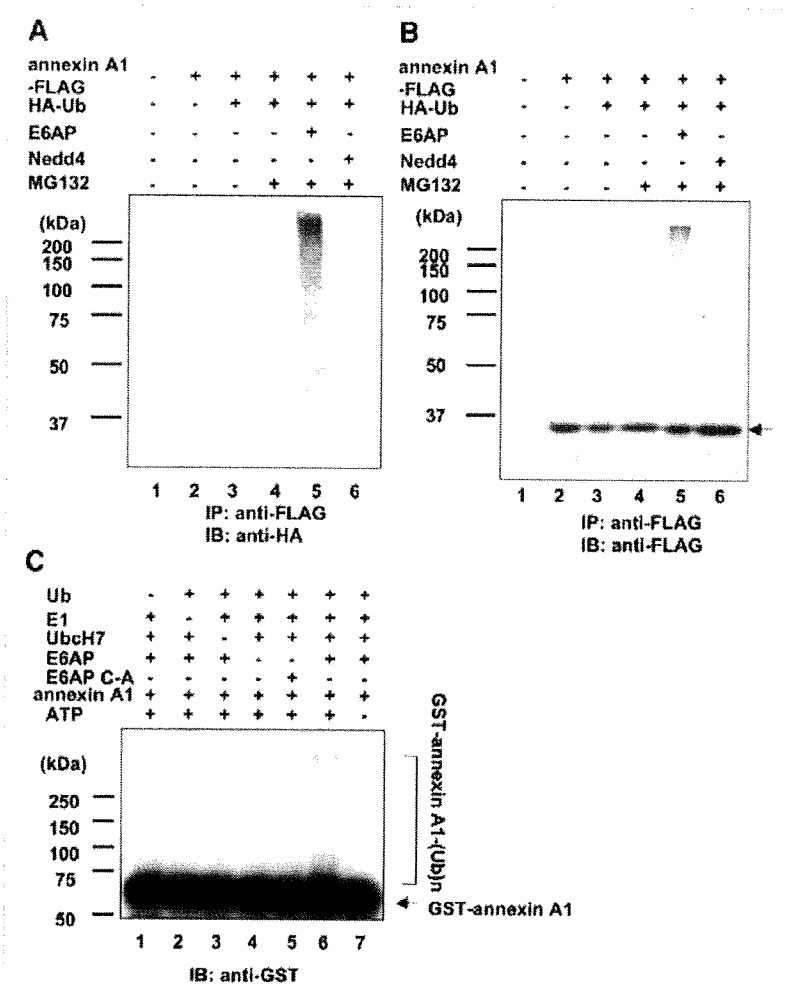

Fig. 5. E6AP-dependent ubiquitylation of annexin A1 protein in vivo and in vitro. HEK 293T cells (1×10^6 cells/10-cm dish) were transfected with 1 μg of pCAG annexin-FLAG together with 2 μg of plasmid encoding E6AP as indicated. Each transfection also included 2 μg of plasmid encoding HA-ubiquitin. The cell lysates were immunoprecipitated with FLAG beads and analyzed by immunoblotting with anti-HA PAb (A) or anti-FLAG PAb (B). The Western blot shows the presence of a ubiquitin smear. The arrow indicates annexin-FLAG. IB, immunoblot; IP, immunoprecipitation. C: In vitro ubiquitylation of annexin A1 by E6AP. For in vitro ubiquitylation of annexin A1 protein, purified GST-annexin A1 was used as a substrate. Assays were done in 40-μl volumes containing each component as indicated. The reaction mixture is described in the Experimental Procedures. The reaction mixture contained 1 mM $CaCl_2$. The reaction was terminated by addition of SDS–PAGE loading buffer and followed by immunoblotting with anti-GST PAb. The arrow indicates GST-annexin A1. Ubiquitylated species of GST-annexin A1 proteins are marked by brackets.

In the present study, we have identified annexin A1 as a novel substrate for E6AP using four lines of evidence: (1) E6AP bound to annexin A1 in vivo and in vitro; (2) overexpression of E6AP enhanced proteasomal degradation of annexin A1 in vivo; (3) knockdown of endogenous E6AP by siRNA resulted in the accumulation of endogenous annexin A1 in vivo; and (4) E6AP enhanced the polyubiquitylation of annexin A1 in vivo and in vitro. These results provide evidence that E6AP mediates the ubiquitylation and proteasomal degradation of annexin A1. We have shown that E6AP bound to annexin A1 only in the presence of Ca^{2+} and that these interactions were enhanced by increasing concentrations of Ca^{2+}. Annexin A1 was polyubiquitylated by E6AP only in the presence of Ca^{2+}. Chelating Ca^{2+} with EGTA inhibited E6AP-mediated polyubiquitylation of annexin A1. The E6AP-binding domain on annexin A1 was mapped to the core domain, especially the annexin repeat domain III. These results suggest that the conformational change of annexin A1 induced by Ca^{2+} binding allows E6AP to bind to annexin repeat domain III of annexin A1 and to mediate its ubiquitylation and degradation.

Post-translational modifications, such as Ca^{2+} binding, phosphorylation, and lipidation, have roles in the regulation of annexin A1. Solito et al. [2006] showed that the translocation of annexin A1 from the cytoplasm to the cell surface is regulated by phosphorylation and lipidation. Annexin A1 is phosphorylated by several

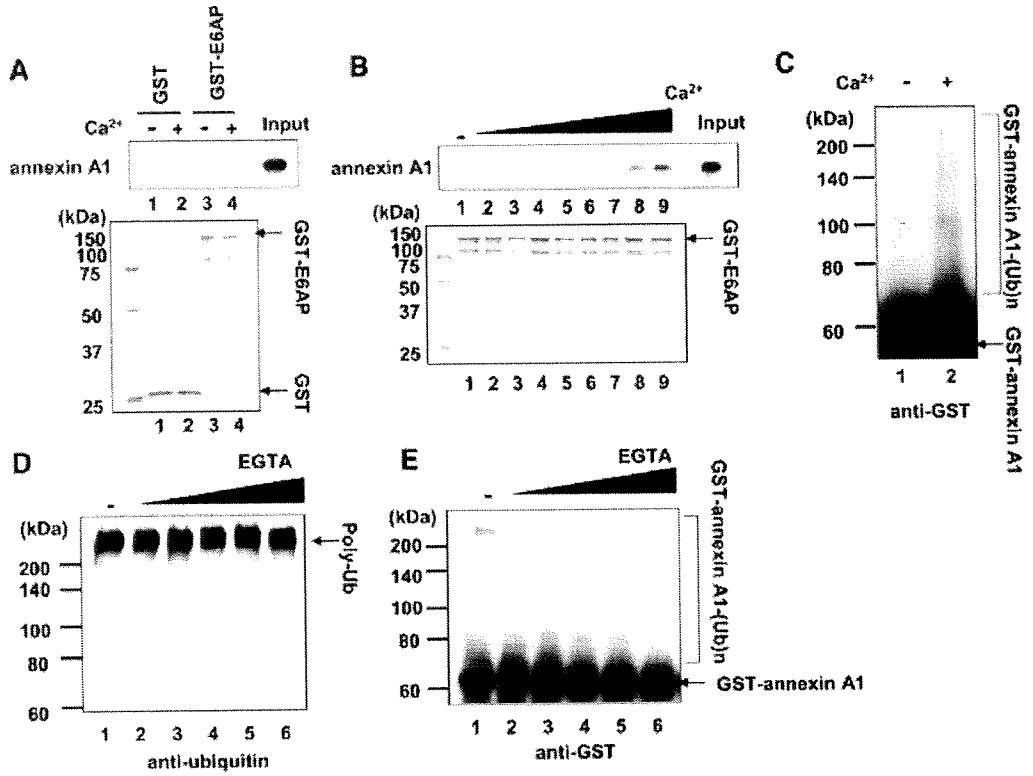

Fig. 6. E6AP mediates ubiquitylation of annexin A1 in a Ca^{2+}-dependent manner. A: In vitro binding of annexin A1 and E6AP. Immobilized GST-E6AP or GST alone was incubated with purified His-annexin A1 in the presence or absence of 1 mM $CaCl_2$ in the binding solution. Immunoblotting to detect bound annexin A1 was performed using anti-annexin A1 antibody. B: Ca^{2+}-dependent interaction between annexin A1 and E6AP. The GST pull-down assays described in (A) were repeated in the presence of increasing concentrations of $CaCl_2$ in the binding solution as follows: lane 1 (0 μM), 2 (10 μM), 3 (100 μM), 4 (250 μM), 5 (500 μM), 6 (750 μM), 7 (1 mM), 8 (2.5 mM), and 9 (5 mM). C: For in vitro ubiquitylation of annexin A1 protein, purified GST-annexin A1 was used as a substrate. Assays were done in 40-μl volumes in the presence or absence of 1 mM $CaCl_2$. The reaction mixture is described in Materials and Methods Section. The reaction was terminated by addition of SDS-PAGE loading buffer and followed by immunoblotting with anti-GST PAb. Arrow indicates GST-annexin A1. Ubiquitylated species of GST-annexin A1 proteins are marked by brackets. D,E: The in vitro ubiquitylation assays were performed in the presence of various concentrations of EGTA in the reaction mixture containing 1 mM $CaCl_2$. The concentrations of EGTA were as follows: lane 1 (0 mM), 2 (0.1 mM), 3 (0.5 mM), 4 (1 mM), 5 (5 mM), and 6 (10 mM). D: Immunoblotting to detect whole polyubiquitylated proteins with anti-ubiquitin MAb. E: Immunoblotting to detect polyubiquitylated GST-annexin A1 with anti-GST PAb.

protein kinases, such as epidermal growth factor receptor protein kinase, protein kinase C, and hepatocyte growth factor receptor kinase to mediate proliferation [Lim and Pervaiz, 2007], suggesting that phosphorylation plays some roles in the regulation of annexin A1 function. The findings presented in this study suggest that the ubiquitin-proteasome pathway plays a role in the regulation of annexin A1 function. Our data also suggest that E6AP preferentially recognizes the Ca^{2+}-binding form of annexin A1 and targets it for proteasomal degradation. The main biological property of annexin A1 is the binding to the phospholipid membrane in a Ca^{2+}-dependent manner [Lim and Pervaiz, 2007]. X-ray crystallography studies of annexin A1 have suggested that a calcium-driven conformational switch of the N-terminal and core domains of annexin A1 involves the membrane aggregation properties of annexin A1 [Rosengarth et al., 2001; Rosengarth and Luecke, 2003]. It will be intriguing to examine the role of E6AP in membrane aggregation. Further investigations will be required to elucidate the role of E6AP in the regulation of annexin A1 functions.

Targeting of a substrate via the ubiquitin system involves specific binding of the protein to the appropriate E3 ubiquitin ligase. There are several modes for specific substrate recognition, such as (1) NH2-terminal residue (N-end rule pathway), (2) allosteric activation, (3) recognition of phosphorylated substrate, (4) phosphorylation of E3, (5) phosphorylation of both the ligase and its substrate, (6) recognition in trans via an ancillary protein, (7) abnormal/mutated/misfolded proteins, and (8) recognition via hydroxylated proline [Glickman and Ciechanover, 2002]. E6AP specifically recognizes active forms of Blk, indicating that tyrosine phosphorylation of the regulatory tyrosine of Blk plays a role in specific substrate recognition [Oda et al., 1999]. Here we propose a novel mechanism of specific substrate recognition in the ubiquitin system, in which E6AP recognizes annexin A1 via a Ca^{2+}-induced conformational change. E6AP plays a direct catalytic role in the

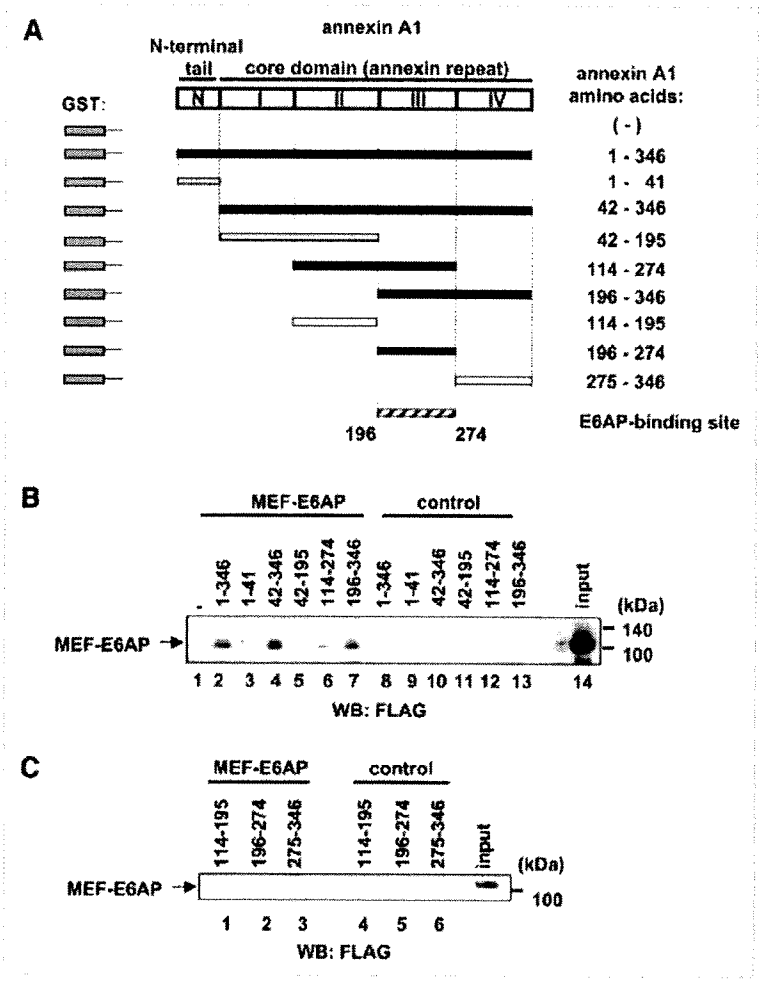

Fig. 7. Mapping of the E6AP-binding domain for annexin A1 protein. A: Structure of annexin A1. Shown is a schematic representation of the region of annexin A1 protein. N-terminal tail (aa 1–41), core domain (aa 42–346), and annexin repeat domains I (aa 42–113), II (aa 114–195), III (aa 196–274), and IV (aa 275–346) are shown. Schematic representation of GST-annexin A1 proteins. GST proteins contain the annexin A1 amino acids indicated to the right. The shaded box in each represents the GST sequence. Closed boxes represent proteins that are bound specifically to MEF-E6AP, and open boxes represent those that are not bound. B,C: In vitro binding of MEF-E6AP to GST-annexin A1 proteins. Purified recombinant MEF-E6AP was assayed for association with GST (−) or the GST-annexin A1 proteins using the binding buffer with 1 mM $CaCl_2$. GST pull-down was performed to assay for the association of E6AP with annexin A1. Control experiments were performed without MEF-E6AP. The association of MEF-E6AP was detected by immunoblotting with anti-FLAG MAb.

final attachment of ubiquitin to substrate proteins. Our findings suggest that Ca^{2+}-induced conformational change of annexin A1 may function as a degradation signal for annexin A1.

Ubiquitylated annexin A2 is enriched in the cytoskeleton fraction of mouse Krebs II cells [Lauvrak et al., 2005]. It remains unclear whether the ubiquitylated annexin A2 is degraded by proteasome. The apical membrane localization of Nedd4, a member of HECT-type ubiquitin ligases, is mediated by an association of its C2 domain with the apically targeted annexin XIIIb [Plant et al., 2000]. However, it is unknown whether annexin XIIIb is a substrate of Nedd4. To our knowledge, this is the first study to identify a specific E3 ubiquitin ligase for the ubiquitylation of an annexin family protein. All annexins share a core domain composed of four similar repeats, each approximately 70 amino acids long. Each repeat is composed of five α helices and usually contains a characteristic type-2 motif for binding calcium ions with the sequence GxGT-[38 residues]-D/E [Moss and Morgan, 2004]. The core domains of most vertebrate annexins reveal conservation of their secondary and tertiary structures despite the presence of only 45–55% amino-acid identity among individual annexins [Moss and Morgan, 2004]. It will be required to investigate whether other annexins are regulated by E6AP or other E3 ubiquitin ligases.

E6AP is hijacked by the HPV16E6 to target the tumor suppressor p53 in cervical cancer. Moreover, E6AP is mutated in Angelman syndrome and mediates ubiquitin-dependent degradation of HCV core protein, suggesting that E6AP plays important roles in sporadic and hereditary human diseases including cancer, neurological disorders, and infectious diseases [Kishino et al., 1997; Scheffner

and Staub, 2007; Shirakura et al., 2007]. Physical and functional association of E6AP with viral proteins, such as HPV16E6 [Huibregtse et al., 1993b] and HCV core protein [Shirakura et al., 2007], have been demonstrated. It is possible that the viral proteins redirect E6AP away from annexin A1, increasing the stability of annexin A1, and thereby contributing to viral pathogenesis. It would be interesting to investigate whether these viral proteins affect E6AP-dependent degradation of annexin A1. The association of E6AP with the viral protein (HPV16E6 or HCV core protein) could provide a feasible target for molecular approaches in the treatment of cervical cancer or HCV-related diseases.

In conclusion, we have demonstrated that E6AP interacts with annexin A1 protein and mediates its ubiquitin-dependent degradation. We propose that E6AP may play a role in regulating the diverse functions of annexin A1 protein. Identification of the specific E3 ubiquitin ligase may provide a link between the annexin family proteins and the ubiquitin-proteasome pathway. Elucidating the regulation of annexin A1 may provide a novel clue in the treatment of the E6AP-related diseases.

ACKNOWLEDGMENTS

We thank Dr. Bohmann (EMBL) for providing pMT123 and Dr. Iwai (Osaka University) for recombinant baculovirus carrying His_6-mouse E1. We also thank S. Yoshizaki, M. Ikeda, and M. Sasaki for technical assistance, and T. Mizoguchi and K. Hachida for secretarial work. This work was supported in part by a grant for Research on Health Sciences focusing on Drug Innovation from the Japan Health Sciences Foundation; by grants-in-aid from the Ministry of Health, Labor, and Welfare; and by the program for Promotion of Fundamental Studies in Health Sciences of the National Institute of Biomedical Innovation (NIBIO), Japan.

REFERENCES

Buckingham JC, John CD, Solito E, Tierney T, Flower RJ, Christian H, Morris J. 2006. Annexin 1, glucocorticoids, and the neuroendocrine-immune interface. Ann NY Acad Sci 1088:396–409.

Ciechanover A. 1998. The ubiquitin-proteasome pathway: On protein death and cell life. EMBO J 17:7151–7160.

Ciechanover A, Heller H, Katz-Etzion R, Hershko A. 1981. Activation of the heat-stable polypeptide of the ATP-dependent proteolytic system. Proc Natl Acad Sci USA 78:761–765.

Ciechanover A, Orian A, Schwartz AL. 2000. Ubiquitin-mediated proteolysis: Biological regulation via destruction. Bioessays 22:442–451.

Cooper EM, Hudson AW, Amos J, Wagstaff J, Howley PM. 2004. Biochemical analysis of Angelman syndrome-associated mutations in the E3 ubiquitin ligase E6-associated protein. J Biol Chem 279:41208–41217.

Gewin L, Myers H, Kiyono T, Galloway DA. 2004. Identification of a novel telomerase repressor that interacts with the human papillomavirus type-16 E6/E6-AP complex. Genes Dev 18:2269–2282.

Glickman MH, Ciechanover A. 2002. The ubiquitin-proteasome proteolytic pathway: Destruction for the sake of construction. Physiol Rev 82:373–428.

Haas AL, Rose IA. 1982. The mechanism of ubiquitin activating enzyme. A kinetic and equilibrium analysis. J Biol Chem 257:10329–10337.

Haigler HT, Schlaepfer DD, Burgess WH. 1987. Characterization of lipocortin I and an immunologically unrelated 33-kDa protein as epidermal growth factor receptor/kinase substrates and phospholipase A2 inhibitors. J Biol Chem 262:6921–6930.

Harris KF, Shoji I, Cooper EM, Kumar S, Oda H, Howley PM. 1999. Ubiquitin-mediated degradation of active Src tyrosine kinase. Proc Natl Acad Sci USA 96:13738–13743.

Hershko A, Ciechanover A. 1998. The ubiquitin system. Annu Rev Biochem 67:425–479.

Hershko A, Heller H, Eytan E, Reiss Y. 1986. The protein substrate binding site of the ubiquitin-protein ligase system. J Biol Chem 261:11992–11999.

Huibregtse JM, Scheffner M, Howley PM. 1993a. Cloning and expression of the cDNA for E6-AP, a protein that mediates the interaction of the human papillomavirus E6 oncoprotein with p53. Mol Cell Biol 13:775–784.

Huibregtse JM, Scheffner M, Howley PM. 1993b. Localization of the E6-AP regions that direct human papillomavirus E6 binding, association with p53, and ubiquitination of associated proteins. Mol Cell Biol 13:4918–4927.

Huibregtse JM, Scheffner M, Beaudenon S, Howley PM. 1995. A family of proteins structurally and functionally related to the E6-AP ubiquitin-protein ligase. Proc Natl Acad Sci USA 92:2563–2567.

Kaji H, Tsuji T, Mawuenyega KG, Wakamiya A, Taoka M, Isobe T. 2000. Profiling of Caenorhabditis elegans proteins using two-dimensional gel electrophoresis and matrix assisted laser desorption/ionization-time of flight-mass spectrometry. Electrophoresis 21:1755–1765.

Kao WH, Beaudenon SL, Talis AL, Huibregtse JM, Howley PM. 2000. Human papillomavirus type 16 E6 induces self-ubiquitination of the E6AP ubiquitin-protein ligase. J Virol 74:6408–6417.

Kelley ML, Keiger KE, Lee CJ, Huibregtse JM. 2005. The global transcriptional effects of the human papillomavirus E6 protein in cervical carcinoma cell lines are mediated by the E6AP ubiquitin ligase. J Virol 79:3737–3747.

Kishino T, Lalande M, Wagstaff J. 1997. UBE3A/E6-AP mutations cause Angelman syndrome. Nat Genet 15:70–73.

Kuhne C, Banks L. 1998. E3-ubiquitin ligase/E6-AP links multicopy maintenance protein 7 to the ubiquitination pathway by a novel motif, the L2G box. J Biol Chem 273:34302–34309.

Kumar S, Talis AL, Howley PM. 1999. Identification of HHR23A as a substrate for E6-associated protein-mediated ubiquitination. J Biol Chem 274:18785–18792.

Lauvrak SU, Hollas H, Doskeland AP, Aukrust I, Flatmark T, Vedeler A. 2005. Ubiquitinated annexin A2 is enriched in the cytoskeleton fraction. FEBS Lett 579:203–206.

Lim LH, Pervaiz S. 2007. Annexin 1: The new face of an old molecule. FASEB J 21:968–975.

Mani A, Oh AS, Bowden ET, Lahusen T, Lorick KL, Weissman AM, Schlegel R, Wellstein A, Riegel AT. 2006. E6AP mediates regulated proteasomal degradation of the nuclear receptor coactivator amplified in breast cancer 1 in immortalized cells. Cancer Res 66:8680–8686.

Moss SE, Morgan RO. 2004. The annexins. Genome Biol 5:219.

Nakagawa S, Huibregtse JM. 2000. Human scribble (Vartul) is targeted for ubiquitin-mediated degradation by the high-risk papillomavirus E6 proteins and the E6AP ubiquitin-protein ligase. Mol Cell Biol 20:8244–8253.

Niwa H, Yamamura K, Miyazaki J. 1991. Efficient selection for high-expression transfectants with a novel eukaryotic vector. Gene 108:193–199.

Oda H, Kumar S, Howley PM. 1999. Regulation of the Src family tyrosine kinase Blk through E6AP-mediated ubiquitination. Proc Natl Acad Sci USA 96:9557–9562.

Oudinet JP, Russo-Marie F, Cavadore JC, Rothhut B. 1993. Protein kinase C-dependent phosphorylation of annexins I and II in mesangial cells. Biochem J 292(Pt 1):63–68.

Plant PJ, Lafont F, Lecat S, Verkade P, Simons K, Rotin D. 2000. Apical membrane targeting of Nedd4 is mediated by an association of its C2 domain with annexin XIIIb. J Cell Biol 149:1473–1484.

Rosengarth A, Luecke H. 2003. A calcium-driven conformational switch of the N-terminal and core domains of annexin A1. J Mol Biol 326:1317–1325.

Rosengarth A, Gerke V, Luecke H. 2001. X-ray structure of full-length annexin 1 and implications for membrane aggregation. J Mol Biol 306: 489–498.

Scheffner M, Staub O. 2007. HECT E3s and human disease. BMC Biochem 8 (Suppl 1): S6.

Scheffner M, Huibregtse JM, Vierstra RD, Howley PM. 1993. The HPV-16 E6 and E6-AP complex functions as a ubiquitin-protein ligase in the ubiquitination of p53. Cell 75:495–505.

Scheffner M, Huibregtse JM, Howley PM. 1994. Identification of a human ubiquitin-conjugating enzyme that mediates the E6-AP-dependent ubiquitination of p53. Proc Natl Acad Sci USA 91:8797–8801.

Shirakura M, Murakami K, Ichimura T, Suzuki R, Shimoji T, Fukuda K, Abe K, Sato S, Fukasawa M, Yamakawa Y, Nishijima M, Moriishi K, Matsuura Y, Wakita T, Suzuki T, Howley PM, Miyamura T, Shoji I. 2007. E6AP ubiquitin ligase mediates ubiquitylation and degradation of hepatitis C virus core protein. J Virol 81:1174–1185.

Skouteris GG, Schroder CH. 1996. The hepatocyte growth factor receptor kinase-mediated phosphorylation of lipocortin-1 transduces the proliferating signal of the hepatocyte growth factor. J Biol Chem 271:27266–27273.

Solito E, Christian HC, Festa M, Mulla A, Tierney T, Flower RJ, Buckingham JC. 2006. Post-translational modification plays an essential role in the translocation of annexin A1 from the cytoplasm to the cell surface. FASEB J 20:1498–1500.

Staub O, Dho S, Henry P, Correa J, Ishikawa T, McGlade J, Rotin D. 1996. WW domains of Nedd4 bind to the proline-rich PY motifs in the epithelial Na+ channel deleted in Liddle's syndrome. EMBO J 15:2371–2380.

Talis AL, Huibregtse JM, Howley PM. 1998. The role of E6AP in the regulation of p53 protein levels in human papillomavirus (HPV)-positive and HPV-negative cells. J Biol Chem 273:6439–6445.

Varticovski L, Chahwala SB, Whitman M, Cantley L, Schindler D, Chow EP, Sinclair LK, Pepinsky RB. 1988. Location of sites in human lipocortin I that are phosphorylated by protein tyrosine kinases and protein kinases A and C. Biochemistry 27:3682–3690.

Yang Y, Liu W, Zou W, Wang H, Zong H, Jiang J, Wang Y, Gu J. 2007. Ubiquitin-dependent proteolysis of trihydrophobin 1 (TH1) by the human papilloma virus E6-associated protein (E6-AP). J Cell Biochem 101:167–180.

Journal of General Virology (2009), 90, 1681–1691 DOI 10.1099/vir.0.010983-0

Efficient production of infectious hepatitis C virus with adaptive mutations in cultured hepatoma cells

Yasuaki Bungyoku, Ikuo Shoji, Tatsuhiko Makine, Tetsuya Adachi, Kazumi Hayashida, Motoko Nagano-Fujii, Yoshi-Hiro Ide, Lin Deng and Hak Hotta

Correspondence
Hak Hotta
hotta@med.kobe-u.ac.jp

Division of Microbiology, Kobe University Graduate School of Medicine, 7-5-1 Kusunoki-cho, Chuo-ku, Kobe, Hyogo 650-0017, Japan

Robust production of infectious hepatitis C virus (HCV) in cell culture was realized by using the JFH1 strain and the homologous chimeric J6/JFH1 strain in Huh-7.5 cells, a highly HCV-permissive subclone of Huh-7 cells. In this study, we aimed to establish a more efficient HCV-production system and to gain some insight into the adaptation mechanisms of efficient HCV production. By serial passaging of J6/JFH1-infected Huh-7.5 cells, we obtained culture-adapted J6/JFH1 variants, designated P-27, P-38 and P-47. Sequence analyses revealed that the adaptive mutant viruses P-27, P-38 and P-47 possessed eight mutations [four in E2, two in NS2, one in NS5A and one in NS5B), 10 mutations [two additional mutations in the 5′-untranslated region (5′-UTR) and core] and 11 mutations (three additional mutations in 5′-UTR, core and NS5B), respectively. We introduced amino acid substitutions into the wild-type J6/JFH1 clone, generated recombinant viruses with adaptive mutations and analysed their infectivity and ability to produce infectious viruses. The viruses with the adaptive mutations exhibited higher expression of HCV proteins than did the wild type in Huh-7.5 cells. Moreover, we provide evidence suggesting that the mutation N534H in the E2 glycoprotein of the mutant viruses conferred an advantage at the entry level. We thus demonstrate that an efficient HCV-production system could be obtained by introducing adaptive mutations into the J6/JFH1 genome. The J6/JFH1-derived mutant viruses presented here would be a good tool for producing HCV particles with enhanced infectivity and for studying the molecular mechanism of HCV entry.

Received 11 February 2009
Accepted 5 March 2009

INTRODUCTION

Hepatitis C virus (HCV) is the main cause of chronic hepatitis, liver cirrhosis and hepatocellular carcinoma (Choo *et al.*, 1989; Kuo *et al.*, 1989; Saito *et al.*, 1990). As more than 170 million people worldwide are infected chronically with HCV (Poynard *et al.*, 2003) and because the current antiviral therapy, interferon and ribavirin, produces sustained virus clearance in <50 % of treated patients (Manns *et al.*, 2007), HCV infection is clearly a problem of major proportions. HCV is a single-stranded, positive-sense RNA virus that is classified in the genus *Hepacivirus* in the family *Flaviviridae*. The approximately 9.6 kb HCV genome encodes one large open reading frame (ORF) that is flanked at the 5′ and 3′ ends by untranslated regions (UTRs) (Choo *et al.*, 1991). The HCV polyprotein is processed into at least 10 proteins by viral proteases and cellular signalases (Grakoui *et al.*, 1993; Hijikata *et al.*, 1993a; McLauchlan *et al.*, 2002). The structural proteins core, E1 and E2 are located in the N terminus of the polyprotein, followed by p7 and the non-structural (NS) proteins NS2, NS3, NS4A, NS4B, NS5A and NS5B (Bartenschlager & Sparacio, 2007).

Study of the HCV life cycle and virus–host interaction has been hampered severely by the lack of a robust *in vitro* cell-culture system and small-animal models of HCV infection (Bartenschlager & Sparacio, 2007). The development of HCV replicon systems has made an important contribution to the study of HCV translation and RNA replication in the human hepatoma cell line Huh-7 (Blight *et al.*, 2000; Lohmann *et al.*, 1999). Sequence analyses of multiple HCV replicons have revealed that several adaptive mutations enhance RNA replication to varying degrees (Bartenschlager & Sparacio, 2007; Blight *et al.*, 2000; Lohmann *et al.*, 2001). Such adaptive mutations were primarily identified in a central portion of the NS5A protein. Although the extent to which these adaptive mutations enhance RNA replication was subsequently studied by using various transient replication assays, the molecular mechanism underlying replication enhancement still remains elusive (Bartenschlager & Sparacio, 2007). The HCV replicons containing adaptive mutations do not produce infectious virus particles in culture and are severely attenuated (Blight *et al.*, 2002; Pietschmann *et al.*, 2002). Using recombinant HCV envelope glycoproteins

and HCV pseudoparticles, several cell-surface molecules have been shown to interact with HCV during virus binding and entry, including the tetraspanin CD81 (Bartosch *et al.*, 2003; Pileri *et al.*, 1998), the scavenger receptor class B member I (SR-BI) (Bartosch *et al.*, 2003; Scarselli *et al.*, 2002) and the tight junction protein claudin-1 (CLDN1) (Evans *et al.*, 2007).

The major breakthrough was made by establishing an HCV-production system using HCV strain JFH1, a genotype 2a isolate, and Huh-7 cells (Wakita *et al.*, 2005). Two other groups reported a robust production of infectious virus using a homologous chimeric FL-J6/JFH1 strain (Lindenbach *et al.*, 2005) or using Huh-7.5.1 cells (Zhong *et al.*, 2005) derived from the cell line Huh-7.5, which has a defect in the RIG-I pathway (Sumpter *et al.*, 2005). Upon transfection of Huh-7 cells with the *in vitro*-transcribed HCV JFH1 genome or the chimera FL-J6/JFH1, infectious HCV particles were secreted in an envelope glycoprotein-dependent manner (Lindenbach *et al.*, 2005; Wakita *et al.*, 2005; Zhong *et al.*, 2005). Using HCV-production systems, adaptive or compensatory mutations that promote the production of infectious virus from wild-type JFH1 (Delgrange *et al.*, 2007; Kaul *et al.*, 2007; Russell *et al.*, 2008; Zhong *et al.*, 2006) or chimeric viruses (Gottwein *et al.*, 2007; Yi *et al.*, 2006, 2007) have been identified. However, the molecular mechanisms of adaptive mutations are poorly understood.

In this study, we aimed to establish an efficient HCV-production system and to gain more insight into the determinants of efficient virus production. By serial passaging of Huh-7.5 cells infected with the HCV J6/JFH1 strain, we identified adaptive mutations in the clones and analysed the mutations by examining the production of the recombinant mutant viruses.

METHODS

Cell culture. Huh-7.5 cells (Blight *et al.*, 2002), a highly HCV-permissive subclone of Huh-7 cells, were kindly provided by Dr C. M. Rice (Rockefeller University, New York, NY, USA). Cells were cultured in Dulbecco's modified Eagle's medium (DMEM; Wako) supplemented with 10% fetal bovine serum (FBS; Biowest), 0.1 mM non-essential amino acids (Invitrogen), 100 IU penicillin ml^{-1} and 100 μg streptomycin ml^{-1} (Invitrogen). DMEM containing 10% FBS was designated complete DMEM. Cells were grown at 37 °C in a CO_2 incubator.

Antibodies. The mouse monoclonal antibodies (mAbs) used in this study were anti-core (2H9) mAb (Wakita *et al.*, 2005) and anti-HCV NS3 mAb (Chemicon). Goat anti-actin polyclonal antibody (C-11) (Santa Cruz Biotech) was used. Horseradish peroxidase (HRP)-conjugated goat anti-mouse IgG (MBL) and HRP-conjugated donkey anti-goat IgG (Santa Cruz Biotech) were used as secondary antibodies.

Plasmids. Plasmid pFL-J6/JFH1 (Lindenbach *et al.*, 2005) containing the full-length chimeric HCV genome was used to generate infectious HCV. Amino acid substitutions were introduced by site-directed mutagenesis using a QuikChange site-directed mutagenesis kit (Stratagene). All PCR-amplified DNA fragments were verified extensively by using an ABI PRISM 3100-Avant Genetic Analyzer (Applied Biosystems). The primer sequences used in this study are available from the authors upon request.

HCV RNA transfection and virus production. The pFL-J6/JFH1 plasmid was linearized with *Xba*I and *in vitro*-transcribed by using the T7 RiboMAX Express large-scale RNA production system (Promega) following the manufacturer's instructions. The quality of synthesized RNA was examined by agarose gel electrophoresis. Cells were trypsinized and washed with serum-free DMEM. In total, 6×10^6 cells were suspended in 500 μl serum-free DMEM and mixed with 10 μg *in vitro*-transcribed RNA in a 4 mm cuvette (Bio-Rad). The synthesized RNA was introduced into Huh-7.5 cells by electroporation using a Bio-Rad Gene Pulser system with a single pulse at 270 V, 975 μF. The cells were then plated in 10 cm culture dishes containing complete DMEM.

Indirect immunofluorescence. Immunofluorescence staining was performed essentially as described previously (Takigawa *et al.*, 2004). Cells seeded on glass coverslips in a 24-well plate at a density of 4×10^4 cells per well were infected with HCV. Cells were cultured, washed with PBS and fixed with 3.7% paraformaldehyde in PBS for 10 min at room temperature, followed by permeabilization in 0.1% Triton X-100 in PBS for 10 min at room temperature. After being washed twice with PBS, cells were blocked with 5% goat serum in PBS and then incubated with the serum of an HCV-infected patient with a high titre of anti-HCV antibodies. Fluorescein isothiocyanate-conjugated goat anti-human IgG (MBL) was used as a secondary antibody. The cells were washed with PBS, counterstained with Hoechst 33342 solution (Molecular Probes) at room temperature for 10 min, mounted on glass slides and examined under a fluorescence microscope (BX51; Olympus).

Virus titration. Culture supernatants were diluted serially 10-fold in complete DMEM and used to infect 2×10^5 naïve Huh-7.5 cells per well in 24-well plates. The inoculum was incubated with cells for 6 h at 37 °C and then supplemented with fresh complete DMEM. The level of HCV infection was determined 1 day post-infection by immunofluorescence using anti-HCV polyclonal antibody. The virus titre was expressed in focus-forming units (ml supernatant)$^{-1}$ (f.f.u. ml^{-1}), as determined by the mean number of HCV-positive foci detected at the highest dilutions according to a previously described method (Zhong *et al.*, 2005).

Immunoblotting. Immunoblotting was performed essentially as described previously (Muramatsu *et al.*, 1997). To detect the expression of HCV proteins, the immune complexes were visualized by an ECL Western blotting detection kit (GE Healthcare) following the manufacturer's instructions.

HCV RNA quantification. Total RNA was extracted by using RNAiso (TaKaRa) according to the manufacturer's instructions. One microgram of isolated RNA was reverse-transcribed by using a QuantiTect reverse transcription kit (Qiagen) with random primers. RT-qPCR analysis was performed as described previously (Zhong *et al.*, 2005). HCV RNA was monitored by using the PCR primers 5′-TCTGCGGAACCGGTGAGTA-3′ (sense) and 5′-TCAGGCAGTACCACAAGGC-3′ (antisense). HCV transcript levels were determined relative to a standard curve comprising serial dilutions of plasmid containing the HCV J6/JFH1 cDNA.

HCV RNA genome sequencing. HCV RNA was isolated from 140 μl viral supernatant by using a QIAamp Viral RNA Mini kit (Qiagen), and then used as a template to generate cDNA in a reverse-transcription reaction using SuperScript One-Step RT-PCR with Platinum *Taq* (Invitrogen) according to the manufacturer's instruc-

tions. PCR primers of between 20 and 26 bases, designed using the sequence of J6/JFH1, were used to amplify four fragments of HCV cDNA (nt 49–3517, 2582–5966, 5832–8038 and 7870–9286) to cover most of the HCV genome. In addition, the 5′-end sequence was amplified by using the 5′ RACE System for Rapid Amplification of cDNA Ends (Invitrogen) and the 3′-end sequence was amplified by using a 3′-Full RACE Core set (TaKaRa). The sequences of the amplified DNA were determined by using an ABI PRISM 3100-Avant Genetic Analyzer.

Quantification of HCV core protein. HCV core protein in the cells or cell-culture supernatants was quantified by using a highly sensitive enzyme immunoassay (Ortho HCV antigen ELISA kit; Ortho Clinical Diagnostics). To determine intracellular amounts of core, cell lysates were prepared as described by Schaller *et al.* (2007).

Blocking of virus attachment and entry with anti-CD81 antibody. Blocking of virus attachment and entry with anti-CD81 antibody was performed essentially as described previously (Wakita *et al.*, 2005). Huh-7.5 cells (6×10^4 cells per 24-well plate) were pretreated with anti-CD81 antibody (clone JS-81; BD Biosciences) or an isotype-matched control antibody (purified mouse IgG1, κ isotype control; BD Biosciences) as indicated for 1 h. Cells were then infected with the wild-type or mutant viruses at an m.o.i. of 0.5 or 0.01 for 6 h. The viruses were removed, and the cells were washed with PBS and then supplemented with complete DMEM. The efficiency of infection was monitored 1 day after infection by counting the number of HCV-positive foci by immunofluorescence.

Statistical analysis. A two-tailed Student's *t*-test was applied to evaluate the statistical significance of differences measured from the datasets. A P value of <0.05 was considered to be statistically significant.

RESULTS

Increase in HCV infectivity titres during serial passage

To produce infectious HCV particles, *in vitro*-transcribed genomic J6/JFH1 RNA was electroporated into Huh-7.5 cells. Transfected Huh-7.5 cells were maintained and the infectivity titre of the culture supernatant reached 6×10^4 f.f.u. ml^{-1} at 20 days post-infection. This culture supernatant was designated P-1.

To generate higher infectivity titres for HCV, naïve Huh-7.5 cells (3×10^5 cells per six-well plate) were infected with 1 ml virus stock of P-1 (6×10^4 f.f.u. ml^{-1}) at an m.o.i. of 0.2 and the infected cells were passaged serially every 3–4 days to maintain a subconfluent culture for 6 months. The culture medium was replaced with fresh complete DMEM every day. The extracellular infectivity titres fluctuated in the beginning after transfection and became lowest at the 22nd passage (Fig. 1a). Thereafter, the extracellular infectivity titres increased again and reached highest infectivity at the 47th passage. Therefore, we further examined the supernatants at the 27th, 38th and 47th passages, and the viruses were designated P-27, P-38 and P-47, respectively. The infectivity titres were determined to be 7.0×10^3 f.f.u. ml^{-1} for P-27, 1.7×10^4 f.f.u. ml^{-1} for P-38 and 3.3×10^4 f.f.u. ml^{-1} for P-47 (Fig. 1a). These viruses were used as inocula in the following experiments.

Kinetics of virus production after infection with putative adaptive J6/JFH1 mutants

To examine the virus-production kinetics of these viruses in Huh-7.5 cells, naïve Huh-7.5 cells (3×10^4 cells per 24-well plate) were infected with each inoculum (6×10^3 f.f.u.) at an m.o.i. of 0.2. After infection, the culture supernatants were harvested each day for 10 days and assayed for infectivity titres (Fig. 1b). The P-1 virus showed a peak infectivity titre of 2.3×10^4 f.f.u. ml^{-1} at 4 days post-infection, whereas the P-27, P-38 and P-47 viruses showed peak titres of 1.0×10^6, 2.3×10^6 and 6.0×10^6 f.f.u. ml^{-1} at 4–5 days post-infection, respectively (Fig. 1b), suggesting that these three viruses produce infectious HCV particles more efficiently than the P-1 virus. The increased infectivity titres may have been due to an increase in the absolute number of released HCV particles or an increased proportion of infectious relative to non-infectious particles. To address this question, we compared the specific infectivities of the mutant viruses with those of the wild-type virus. The ratio of viral infectivity titre (f.f.u. ml^{-1}) to HCV RNA content [genome equivalents (GE) ml^{-1}] was determined as shown in Table 1. The mutant viruses, P-27, P-38 and P-47, had higher specific-infectivity titres (1 : 21, 1 : 10 and 1 : 10, respectively) than the wild-type virus P-1 (1 : 133), suggesting that the mutant viruses are more infectious than the wild type and that the mutant viruses possess adaptive mutations in the virus genomes.

Sequence analysis of genetic mutations in the adaptive mutants

To identify the genetic changes in the virus genomes that are responsible for the adaptation to Huh-7.5 cells, we sequenced the whole genomes of the viruses. No mutation was found in the P-1 virus, whereas several mutations were identified in the P-27, P-38 and P-47 viruses (Fig. 1c). The sequencing analysis of P-27 identified eight mutations that were located in the E2, NS2, NS5A and NS5B regions as follows: T396A, T416A, N534H and A712V in E2; Y852H and W879R in NS2; F2281L in NS5A; and M2876L in NS5B (Fig. 1c). P-38 possessed 10 mutations, the same mutations as in P-27 and two additional mutations. The additional mutations were found at nucleotide position 146 (U to A) in the 5′-UTR and an amino acid change, K78E, in the core region. P-47 contained 11 mutations, including the same 10 mutations as P-38 and one additional mutation, T2925A in NS5B. Thus, the first eight mutations were all present in the genomes of the three viruses, and the results suggested that these eight mutations contribute to the enhanced infectivity.

Effects of individual mutations on the production of infectious HCV

To determine which mutation is responsible for the enhancement of infectivity, recombinant genomes containing only one of the selected mutations were constructed

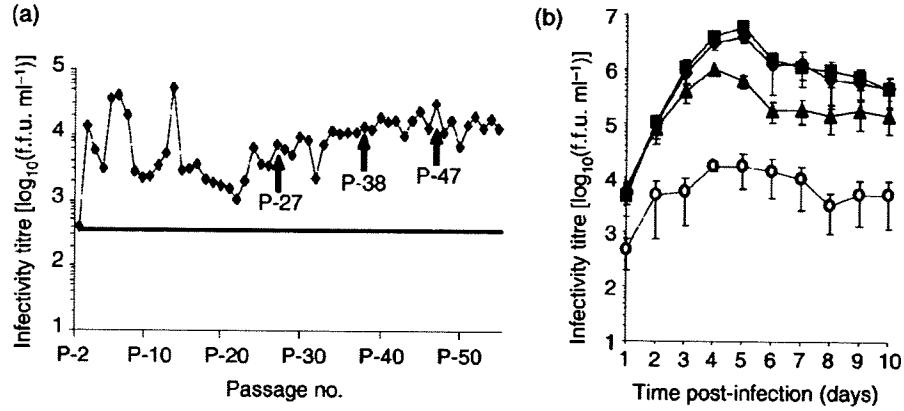

(c)

Virus	Position changed										
	5'-UTR	Core	E2				NS2		NS5A	NS5B	
	(nt 146)	78	396	416	534	712	852	879	2281	2876	2925
Wild-type	U	Lys	Thr	Thr	Asn	Ala	Tyr	Trp	Phe	Met	Thr
P-1	–	–	–	–	–	–	–	–	–	–	–
P-27	–	–	Ala	Ala	His	Val	His	Arg	Leu	Leu	–
P-38	A	Glu	Ala	Ala	His	Val	His	Arg	Leu	Leu	–
P-47	A	Glu	Ala	Ala	His	Val	His	Arg	Leu	Leu	Ala

Fig. 1. Increase in HCV infectivity titres during serial passage. (a) Serial passage of HCV J6/JFH1-infected Huh-7.5 cells. Huh-7.5 cells (3×10^5 cells per six-well plate) were infected with 1 ml stock of wild-type J6/JFH1 virus (P-1) (6×10^4 f.f.u. ml^{-1}) at an m.o.i. of 0.2, and the infected cells were passaged serially every 3–4 days to maintain a subconfluent culture for 6 months. The culture medium was replaced with fresh complete DMEM each day. The extracellular infectivity titres were determined by titration assay and are expressed as f.f.u. ml^{-1}. Arrows show the time points at which we collected the putative adapted viruses, designated P-27, P-38 and P-47. (b) Kinetics of virus production after infection with putative J6/JFH1 adaptive mutants in Huh-7.5 cells. Huh-7.5 cells were infected with the wild-type J6/JFH1 virus (○, P-1) or putative adaptive mutants (▲, P-27; ◆, P-38; ■, P-47) at an m.o.i. of 0.2. After infection, the culture supernatants were harvested every day until 10 days post-infection. Infectivity titres were measured by immunofluorescence assay and are expressed as f.f.u. ml^{-1}. Error bars represent SD for triplicate measurements. (c) Genetic mutations identified during passage. Numbers indicate the amino acid position where mutations were identified. The nucleotide position with mutation is given in parentheses.

(Fig. 2a). The *in vitro*-transcribed mutant J6/JFH1 RNAs were electroporated into Huh-7.5 cells and mutant viruses were generated. Then, naïve Huh-7.5 cells were infected with each virus at an m.o.i. of 0.01 and cultured for 12 days. The culture supernatant was collected every day from 1 to 12 days post-infection. The ability of each mutant virus to release infectious virus particles was examined by titration assay. As shown in Fig. 2(b), the recombinant viruses with single point mutations did not enhance the production of infectious virus particles, suggesting that a single point mutation is not enough for the enhanced infectivity.

Table 1. Specific-infectivity titres of the adaptive J6/JFH1 mutant viruses

Virus	HCV RNA copies [$\log_{10}$(GE ml^{-1})]	Infectivity titre [$\log_{10}$(f.f.u. ml^{-1})]	Specific infectivity (f.f.u.:GE)
P-1	6.7±0.1	4.6±0.1	1:133
P-27	7.3±0.1	6.0±0.2	1:21
P-38	7.4±0.1	6.4±0.0	1:10
P-47	7.3±0.1	6.3±0.2	1:10

Effects of combination of adaptive mutations on the production of infectious HCV

We then generated recombinant viruses with several mutations, as shown in Fig. 3(a). Naïve Huh-7.5 cells were infected with each virus at an m.o.i. of 0.01 and cultured for 12 days. The culture supernatant was collected every day from 1 to 12 days post-infection. The ability of each mutant virus to release infectious virus particles was examined by titration assay. The R-27, R-38 and R-47 viruses reached higher titres than the wild type and other mutant viruses, suggesting that all of the mutations in E2, NS2, NS5A and NS5B were important for the enhancement of infectivity (Fig. 3b). To determine the specific infectivities of the mutant viruses, the ratio of the viral infectivity titre (f.f.u. ml^{-1}) to the HCV RNA content (GE

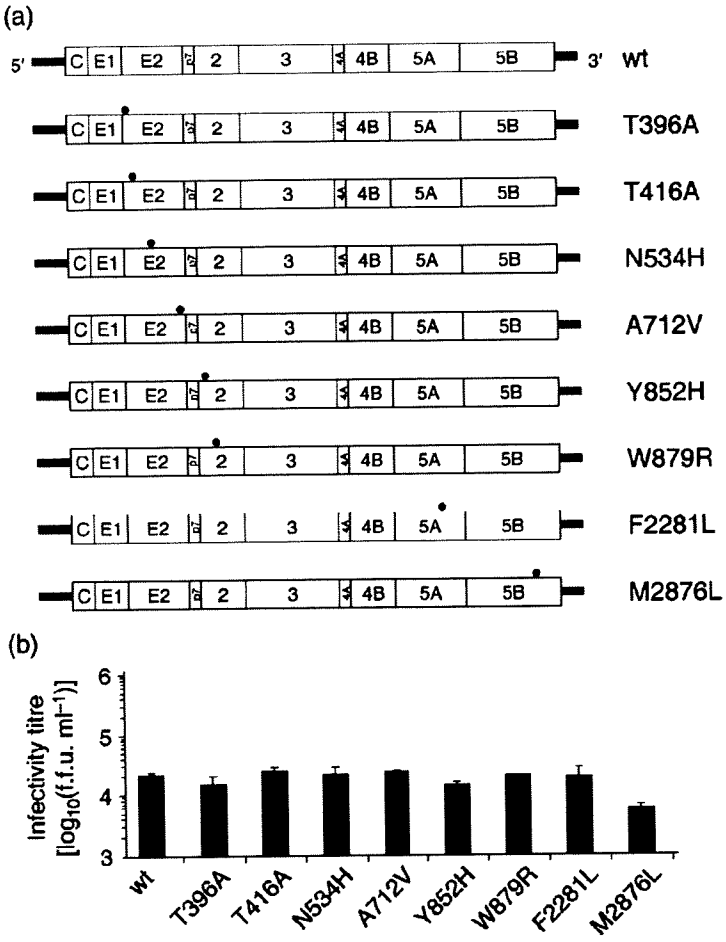

Fig. 2. Effects of individual mutations on the production of infectious HCV. (a) Schematic representation of the wild-type (wt) and mutant chimeric HCV J6/JFH1 genomes. HCV J6/JFH1 mutants with a single point mutation are shown. The adaptive mutations T396A, T416A, N534H, A712V, Y852H, W879R, F2281L and M2876L are indicated by ●. (b) The *in vitro*-transcribed mutant J6/JFH1 RNAs were electroporated into Huh-7.5 cells to generate recombinant mutant viruses. The infectivity titres of the culture supernatants were measured by titration assay. Then, naïve Huh-7.5 cells were infected with each virus at an m.o.i. of 0.01 and cultured for 12 days. The culture supernatant was collected every day from 1 to 12 days post-infection. The ability of each mutant virus to release infectious virus particles was examined by titration assay. Infectivity titres reached maximal levels at 10 days post-infection and the maximal infectivity titres were plotted. Error bars represent SD for triplicate measurements.

ml^{-1}) was calculated as shown in Table 2. The recombinant mutant viruses, R-27, R-38 and R-47, had higher specific-infectivity titres (1:46, 1:35 and 1:54, respectively) than the wild-type virus P-1 (1:197), suggesting that the particles released from cells infected with the R-27, R-38 and R-47 viruses are more infectious than those released from cells infected with the wild-type J6/JFH1 virus.

Efficient expression of HCV proteins in Huh-7.5 cells infected with the adaptive mutants

To investigate further the mechanism of adaptive mutations, we performed immunofluorescence staining of the infected cells. Huh-7.5 cells (6×10^4 cells per 24-well plate) were infected with the P-1, R-27, R-38 and R-47 viruses (1.2×10^4 f.f.u.) at an m.o.i. of 0.2. Cells were fixed 5 days post-infection and stained for immunofluorescence. Approximately 90% of the cells were HCV-positive in the P-1-, R-27-, R-38- and R-47-infected cells (Fig. 4a). We next examined protein synthesis by immunoblotting for the HCV core and NS3 proteins. Immunoblot analysis of the cell lysates demonstrated that the levels of the core and NS3 proteins in cells infected with the R-27, R-38 and R-47 viruses were 2.0- to 2.5-fold higher than those in cells infected with the P-1 virus (Fig. 4b, c), suggesting that these mutant viruses have a replicative advantage.

Growth curves of infectious HCV after transfection of RNAs or infection with HCV

To determine whether the replicative advantage is at the level of entry or replication/translation of the genome, we examined one-step growth curves by transfecting equivalent amounts of RNAs of the wild-type and the mutant viruses into Huh-7.5 cells by means of electroporation (Fig. 5a, b). The intracellular and extracellular core protein levels were quantified by core protein-specific ELISA at the indicated times. The one-step growth curves showed that the intracellular and extracellular core protein levels increased with very similar kinetics in the cells transfected with the wild-type and adapted RNAs (Fig. 5a, b).

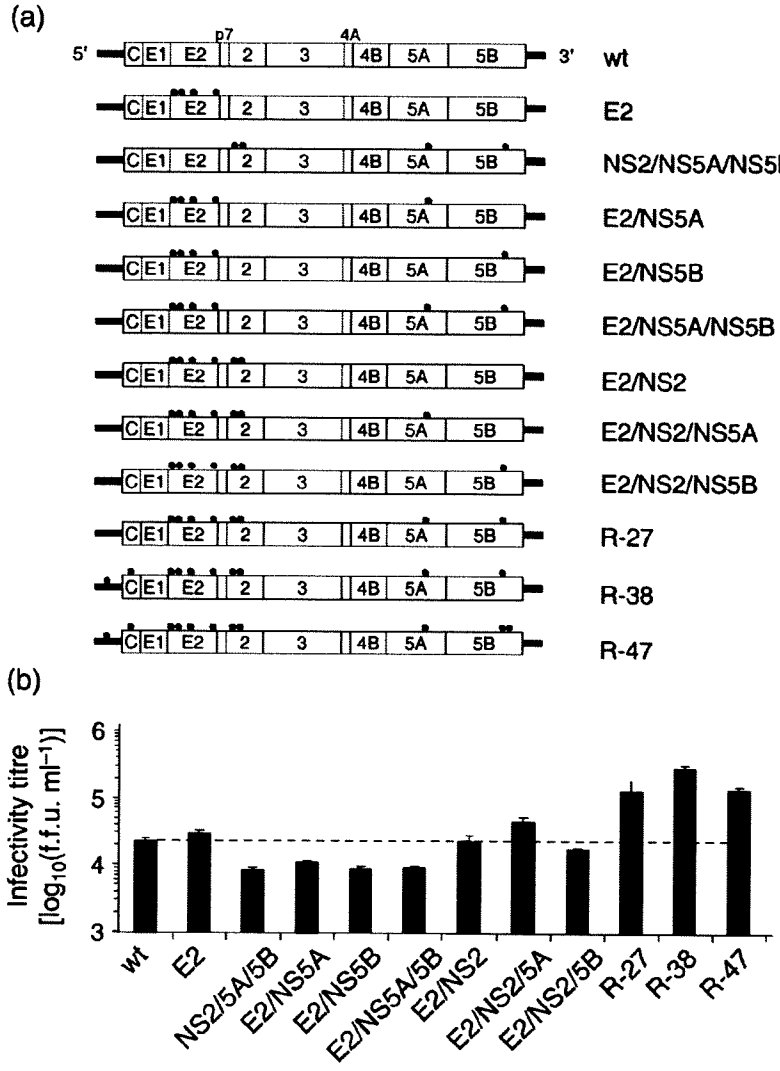

Fig. 3. Effects of combination of adaptive mutations on the production of infectious HCV. (a) Schematic representation of the wild-type (wt) and mutant chimeric HCV J6/JFH1 genomes. The HCV J6/JFH1 genomes with a combination of adaptive mutations at nt 146 (U to A) in the 5'-UTR and amino acid changes at K78E, T396A, T416A, N534H, A712V, Y852H, W879R, F2281L and M2876L are indicated by ●. (b) Recombinant mutant viruses with a combination of mutations were generated. Naïve Huh-7.5 cells were infected with each virus at an m.o.i. of 0.01 and cultured for 12 days. The ability of each mutant to release infectious virus particles was examined by titration assay. Infectivity titres reached maximal levels at 10 or 11 days post-infection and the maximal infectivity titres were plotted. Error bars represent SD for triplicate measurements.

We next examined the growth curves of the core protein levels by infecting cells with the recombinant viruses. The intracellular and extracellular core protein levels in cells infected with the P-1, R-27, R-38 and R-47 viruses were quantified. Huh-7.5 cells (1.2×10^5 cells per 12-well plate) were infected with these viruses at an m.o.i. of 0.2. The intracellular core protein levels in cells infected with the R-27, R-38 and R-47 viruses were 3- to 5-fold higher at day 1 post-infection than those in the P-1-infected cells. The intracellular core protein levels in the cells infected with the mutant viruses were 7- to 11-fold higher at day 3 post-infection than those in the P-1-infected cells (Fig. 5c). The extracellular core protein levels in the P-1-infected cells were comparable to the levels in cells infected with mutant viruses at day 1 post-infection. However, the extracellular core protein levels in cells infected with the R-27, R-38 and R-47 viruses increased more rapidly and reached 4.4- to 5.8-fold higher at day 3 post-infection than those in cells infected with the P-1 virus (Fig. 5d). Taken together, these data suggest that the adaptive mutants have advantages at the entry level, rather than the virus replication/translation level.

Table 2. Specific-infectivity titres of the recombinant adaptive mutant viruses

Virus	HCV RNA copies [$\log_{10}$(GE ml^{-1})]	Infectivity titre [$\log_{10}$(f.f.u. ml^{-1})]	Specific infectivity (f.f.u.:GE)
P-1	6.6±0.1	4.3±0.1	1:197
R-27	6.8±0.1	51±0.2	1:46
R-38	6.9±0	15.4±0.1	1:35
R-47	6.9±0.1	5.1±0.1	1:54

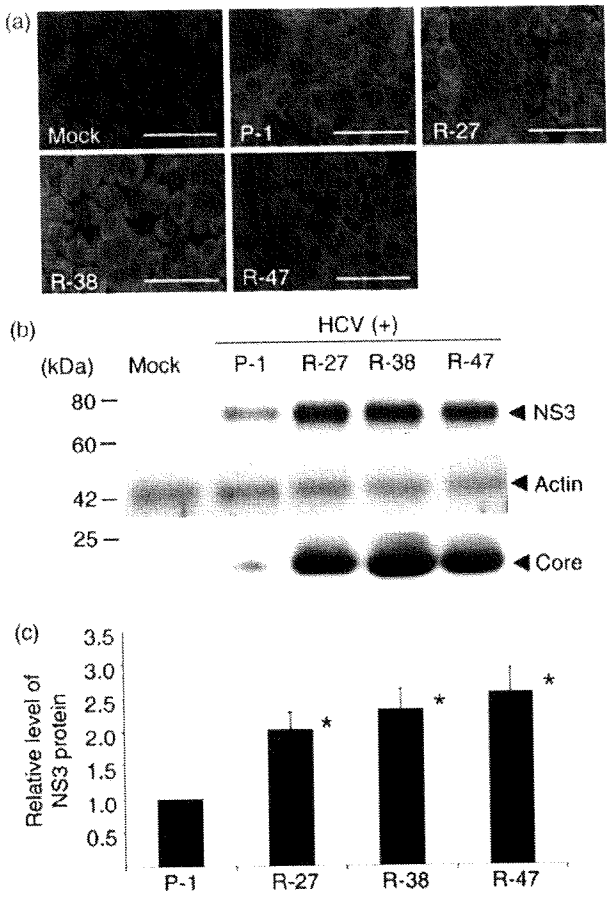

Fig. 4. Efficient expression of HCV proteins in Huh-7.5 cells infected with the adaptive mutants. Huh-7.5 cells (6×10^4 cells per 24-well plate) were infected with 200 µl P-1, R-27, R-38 or R-47 virus (6×10^4 f.f.u. ml^{-1}) at an m.o.i. of 0.2. (a) Cells were fixed 5 days post-infection and stained for immunofluorescence with anti-HCV-positive sera. Bars, 10 µm. (b) Immunoblot analysis of core and NS3 proteins in Huh-7.5 cells infected with R-27, R-38 and R-47 viruses. Data are representative of three independent experiments. (c) Quantification of the data shown in (b). Intensities of the gel bands were quantified by using the Scion Image for Windows program. The level of actin served as a loading control. Error bars represent SD for triplicate measurements. The difference between P-1 and the adaptive mutant (R-27, R-38 or R-47) was significant (*$P<0.05$ by Student's *t*-test).

Blocking of virus attachment and entry with anti-CD81 antibody

To determine whether the adapted mutant viruses have advantages at the entry level, we examined CD81-dependent entry into Huh-7.5 cells. Naïve Huh-7.5 cells were incubated with CD81-specific or non-specific antibody prior to inoculation. We scored infection by immunofluorescence at 24 h post-infection. As shown in Fig. 6(a), the anti-CD81 antibody inhibited the entry of the mutant viruses R-27, R-38 and R-47, as well as the wild-type virus, in a dose-dependent manner, suggesting that interaction between CD81 and HCV E2 glycoprotein is crucial for virus entry for all of these viruses. However, infections by the mutant viruses R-27, R-38 and R-47 were less dependent on CD81 than the wild-type virus. This result suggests that the mutations in the E2 glycoprotein confer an advantage to the mutant viruses at the entry level. We further analysed the mutant viruses to determine which mutation(s) is important for the advantage at the entry level. We infected Huh-7.5 cells with mutant viruses with a single point mutation in the E2 glycoprotein, such as T396A, T416A, N534H or A712V, or with all of the four mutations in E2. Blocking of virus entry with the anti-CD81 antibody was examined as shown in Fig. 6(b). Infection by the mutant virus N534H, as well as the mutant viruses E2, R-27, R-38 and R-47, was less dependent on CD81 than infection by the wild-type virus, whereas the other mutant viruses T396A, T416A and A712V showed a similar pattern to the wild type. These results indicate that the N534H mutation in the E2 region confers an advantage to the adaptive mutant viruses at the entry level.

DISCUSSION

In this study, we established an efficient HCV-production system by serial passaging of Huh-7.5 cells infected with the chimeric HCV J6/JFH1. Sequence analyses revealed that the adapted viruses possessed more than eight non-synonymous mutations in the genomes. Reverse-genetics analysis revealed that the recombinant viruses R-27, R-38 and R-47 exhibited higher expression of the HCV proteins than the wild-type virus. Moreover, we demonstrated that the N534H mutation in the E2 glycoprotein confers an advantage to the mutant viruses at the entry level.

The adaptive mutant viruses possessed four mutations (T396A, T416A, N534H and A712V) in E2. Two of these mutations (T416A and N534H) are in the regions that are involved in E2–CD81 binding and are, therefore, the possible target for neutralizing antibodies inhibiting E2–CD81 interactions (Helle & Dubuisson, 2008). The blocking of virus attachment and entry with CD81-specific antibody in this study revealed that the infections by the E2 R-27, R-38, R-47 and N534H mutants were less dependent on the CD81 molecule than that by the wild type J6/JFH1, suggesting that the N534H mutation gives the mutant viruses a selective advantage at the entry level. The N534H mutation is located in the sixth of 11 *N*-glycosylation sites, and is predicted to remove this *N*-glycosylation. The removal of *N*-glycosylation sites has been shown to have variable effects on CD81 binding and infectivity (Owsianka *et al.*, 2006; Roccasecca *et al.*, 2003). The glycans at positions 417, 532 and 645 (E2N1, E2N6 and E2N11) were shown to reduce the sensitivity of HCV pseudoparticles to antibody neutralization and to reduce the access of CD81 to its binding site on E2 (Goffard *et al.*, 2005). JFH-1 virus with the N534K mutation spread faster than the wild-type

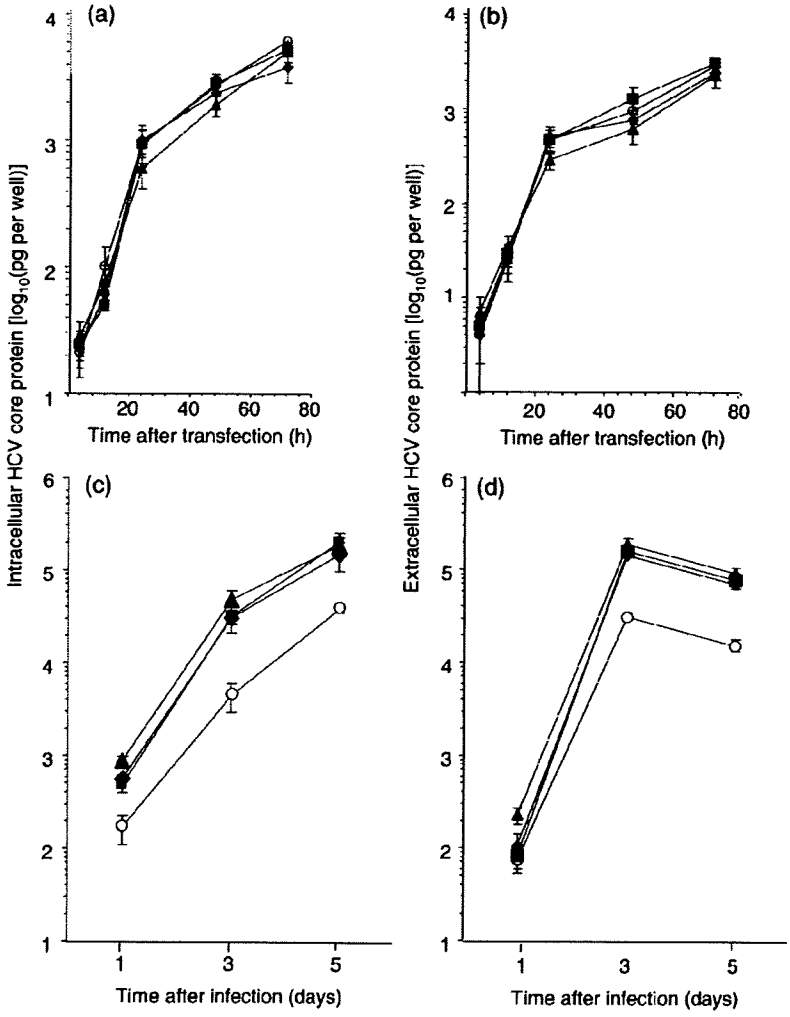

Fig. 5. Effects of adaptive mutations on the production of intracellular and extracellular core protein after transfection of *in vitro*-translated HCV RNAs or after infection of recombinant HCV. (a, b) After electroporation of 10 μg *in vitro*-translated HCV RNAs P-1 (○), R-27 (▲), R-38 (◆) and R-47 (■) into Huh-7.5 cells (5×10^6), the cells were divided into five sets, replated into a six-well plate and cultured. The cells and culture supernatants were harvested at the time points given. Intracellular (a) and extracellular (b) core protein levels were quantified by core protein-specific ELISA. (c, d) After Huh-7.5 cells (1.2×10^5 cells per 12-well plate) were infected with the P-1 (○), R-27 (▲), R-38 (◆) and R-47 (■) viruses at an m.o.i. of 0.2, the cells and culture supernatants were harvested at the time points given. Intracellular (c) and extracellular (d) core protein levels were quantified by core protein-specific ELISA.

JFH-1 virus after two successive amplifications in naïve cells, although the numbers of infectious viruses in the supernatant of transfected cells were initially low (Delgrange *et al.*, 2007). Our results in the growth curves of the viruses in the transfected cells and infected cells were consistent with their report. The CD81 inhibition assay in this study demonstrated clearly that the N534H mutation of the J6/JFH-1 virus confers a selective advantage for J6/JFH-1 at the entry level. To our knowledge, the present study is the first to prove that the mutation at site N534 gives infectious HCV a selective advantage at the entry level. These results raise two possibilities. One is that the N534H mutation in the E2 glycoprotein removes *N*-glycosylation and this mutant E2 glycoprotein possesses a higher affinity for the CD81 molecule, resulting in efficient entry to the cells. Another possibility is that the E2 glycoprotein with the N534H mutation gains higher affinity for other HCV receptors. Further investigation will be required to elucidate the mechanism of this adaptive mutation.

Our results showed that a combination of the mutations in E2, together with four additional mutations in NS2, NS5A and NS5B, resulted in higher infectivity of HCV, suggesting that the additional four mutations possess an advantage at different steps.

NS2 is a membrane-associated cysteine protease (Grakoui *et al.*, 1993; Hijikata *et al.*, 1993b; Lorenz *et al.*, 2006). The N terminus of NS2 consists of one or more transmembrane domains, whilst the C-terminal domain of NS2, together with the N-terminal one-third of NS3, forms the NS2–3 protease, an enzyme that catalyses a single cleavage at the NS2/NS3 boundary. The crystal structure of the C-terminal domain of NS2 has recently been determined and reveals a dimeric protease containing two composite active sites (Lorenz *et al.*, 2006). Jones *et al.* (2007) showed that NS2 and p7 are essential for HCV infectivity. The Y852 and W879 residues are located in the hydrophobic region of NS2. Although the exact topology of NS2 is disputed, the Y852H and W879R mutations would be predicted to lie

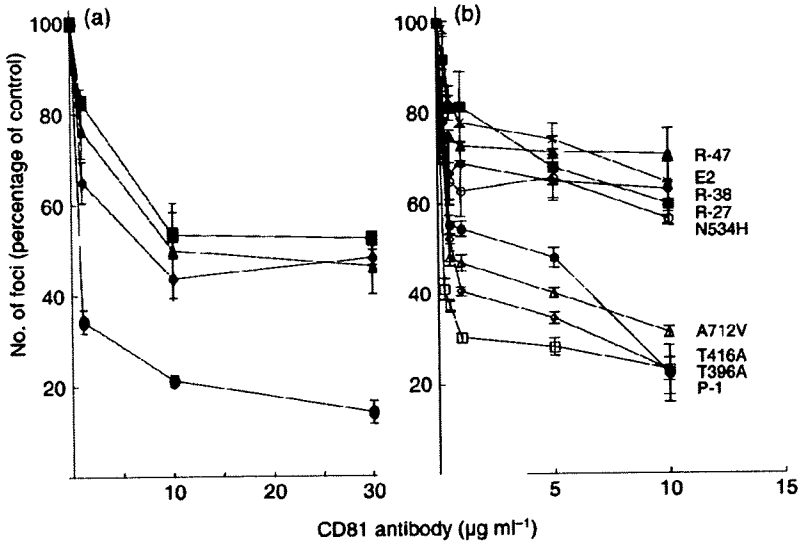

Fig. 6. Blocking of virus attachment and entry with anti-CD81 antibody. (a) Huh-7.5 cells (2×10^5 cells per six-well plate) were pretreated with 0, 1, 10 or 30 μg CD81 antibody (clone JS-81) ml^{-1} for 1 h and then infected with the wild-type (●, P-1) or recombinant mutant (■, R-27; ◆, R-38; ▲, R-47) viruses at an m.o.i. of 0.5. The cells were cultured for 24 h. The infection was monitored by HCV immunofluorescence and the numbers of HCV-positive foci were counted. Each result is expressed as a fraction of the number of foci observed in wells that received the control antibody instead of anti-CD81. Error bars represent SD for triplicate measurements. (b) Huh-7.5 cells (2×10^5 cells per six-well plate) were pretreated with 0, 0.25, 0.5, 1, 5 or 10 μg CD81 antibody ml^{-1} for 1 h and then infected with the wild-type (●, P-1) or recombinant (■, R-27; ◆, R-38; ▲, R-47; ×, E2; □, T396A; ◇, T416A; ○, N534H; △, A712V) viruses at an m.o.i. of 0.01. Blocking of virus entry with anti-CD81 antibody was examined. The infection was monitored by HCV immunofluorescence and the number of HCV-positive foci was counted.

within the second and third transmembrane domains, respectively (Yamaga & Ou, 2002). Murray *et al.* (2007) demonstrated that the A880P mutation increased infectious virus production significantly in the context of the J6/JFH1 genome, suggesting that the mutations in the transmembrane domain of NS2 play an important role in HCV infectivity. It is possible that the Y852H and W879R mutations in the transmembrane domain affect the topology and localization of NS2, and thereby HCV infectivity. Interestingly, NS2 has been found to interact with all other HCV NS proteins in *in vitro* pull-down assays, as well as cell-based colocalization and co-immunoprecipitation experiments (Dimitrova *et al.*, 2003; Hijikata *et al.*, 1993b), suggesting a role for NS2 as part of the replication complex.

Sequence analyses of HCV replicon cells revealed that highly adaptive mutations lie within the NS4B, NS5A and NS5B coding regions, with the majority clustering in NS5A. However, the mechanism underlying the replication enhancement is not known (Bartenschlager & Sparacio, 2007). The mutant viruses possessed an F2281L mutation that was located in domain II of NS5A. NS5A is an RNA-binding phosphoprotein composed of three domains that are separated by trypsin-sensitive low-complexity sequences (LCS I and LCS II) and an N-terminal amphipathic α-helix that anchors the protein stably to intracellular membranes (Brass *et al.*, 2002; Penin *et al.*, 2004; Tellinghuisen *et al.*, 2004). According to the X-ray crystal structure of domain I, it forms a dimer with a claw-like shape that can accommodate a single-stranded RNA molecule (Tellinghuisen *et al.*, 2005). Domain III of NS5A plays an important role in virus assembly and the production of infectious particles (Appel *et al.*, 2008; Masaki *et al.*, 2008; Tellinghuisen *et al.*, 2008). However, the role played by domain II of NS5A in the HCV replication cycle is unknown. Further examination will be required to clarify the effects of the F2281L mutation on the infectivity of the virus. Kaul *et al.* (2007) reported the V2941M mutation in NS5B in the context of the JFH1 genome. Lohmann *et al.* (2001) reported the R2884G mutation in the context of Con1-based replicon cells. Amino acid substitutions within NS5B may favour HCV replication and virus production in ways that remain to be determined.

Miyanari *et al.* (2007) proposed that HCV NS proteins and replication complexes are recruited to lipid droplet-associated membranes by the HCV core protein and that this recruitment is critical for producing infectious viruses. Cholesterol and sphingolipid associated with HCV particles are important for virion maturation and infectivity (Aizaki *et al.*, 2008). We speculate that the additional four mutations in NS2, NS5A and NS5B may confer an advantage in the maturation of virus particles or modification of virus envelopes with cholesterol and sphingolipid. Further investigation will be necessary to elucidate the mechanism of the adaptive mutations in NS2, NS5A and NS5B.

In conclusion, we have developed an efficient HCV-production system by passaging HCV J6/JFH1-infected Huh-7.5 cells. We have demonstrated that an efficient HCV-production system could be obtained by introducing adaptive mutations into the J6/JFH1 genome. The J6/JFH1-derived mutant viruses presented here would be a good tool for producing HCV particles with enhanced infectivity and for studying the molecular mechanism of HCV entry.

ACKNOWLEDGEMENTS

The authors are grateful to Dr C. M. Rice (Center for the Study of Hepatitis C, the Rockefeller University, New York, NY, USA) for providing pFL-J6/JFH1 and Huh-7.5 cells. This work was supported in part by grants-in-aid for Scientific Research from the Ministry of Education, Culture, Sports, Science and Technology (MEXT), and the Ministry of Health, Labour and Welfare, Japan. This study was also carried out as part of the Program of Founding Research Centers for Emerging and Reemerging Infectious Diseases, MEXT, Japan. This study was also part of the Global Center of Excellence (COE) Program at Kobe University Graduate School of Medicine.

REFERENCES

Aizaki, H., Morikawa, K., Fukasawa, M., Hara, H., Inoue, Y., Tani, H., Saito, K., Nishijima, M., Hanada, K. & other authors (2008). Critical role of virion-associated cholesterol and sphingolipid in hepatitis C virus infection. *J Virol* **82**, 5715–5724.

Appel, N., Zayas, M., Miller, S., Krijnse-Locker, J., Schaller, T., Friebe, P., Kallis, S., Engel, U. & Bartenschlager, R. (2008). Essential role of domain III of nonstructural protein 5A for hepatitis C virus infectious particle assembly. *PLoS Pathog* **4**, e1000035.

Bartenschlager, R. & Sparacio, S. (2007). Hepatitis C virus molecular clones and their replication capacity *in vivo* and in cell culture. *Virus Res* **127**, 195–207.

Bartosch, B., Vitelli, A., Granier, C., Goujon, C., Dubuisson, J., Pascale, S., Scarselli, E., Cortese, R., Nicosia, A. & Cosset, F. L. (2003). Cell entry of hepatitis C virus requires a set of co-receptors that include the CD81 tetraspanin and the SR-B1 scavenger receptor. *J Biol Chem* **278**, 41624–41630.

Blight, K. J., Kolykhalov, A. A. & Rice, C. M. (2000). Efficient initiation of HCV RNA replication in cell culture. *Science* **290**, 1972–1974.

Blight, K. J., McKeating, J. A. & Rice, C. M. (2002). Highly permissive cell lines for subgenomic and genomic hepatitis C virus RNA replication. *J Virol* **76**, 13001–13014.

Brass, V., Bieck, E., Montserret, R., Wolk, B., Hellings, J. A., Blum, H. E., Penin, F. & Moradpour, D. (2002). An amino-terminal amphipathic alpha-helix mediates membrane association of the hepatitis C virus nonstructural protein 5A. *J Biol Chem* **277**, 8130–8139.

Choo, Q. L., Kuo, G., Weiner, A. J., Overby, L. R., Bradley, D. W. & Houghton, M. (1989). Isolation of a cDNA clone derived from a blood-borne non-A, non-B viral hepatitis genome. *Science* **244**, 359–362.

Choo, Q. L., Richman, K. H., Han, J. H., Berger, K., Lee, C., Dong, C., Gallegos, C., Coit, D., Medina-Selby, R. & other authors (1991). Genetic organization and diversity of the hepatitis C virus. *Proc Natl Acad Sci U S A* **88**, 2451–2455.

Delgrange, D., Pillez, A., Castelain, S., Cocquerel, L., Rouille, Y., Dubuisson, J., Wakita, T., Duverlie, G. & Wychowski, C. (2007). Robust production of infectious viral particles in Huh-7 cells by introducing mutations in hepatitis C virus structural proteins. *J Gen Virol* **88**, 2495–2503.

Dimitrova, M., Imbert, I., Kieny, M. P. & Schuster, C. (2003). Protein-protein interactions between hepatitis C virus nonstructural proteins. *J Virol* **77**, 5401–5414.

Evans, M. J., von Hahn, T., Tscherne, D. M., Syder, A. J., Panis, M., Wolk, B., Hatziioannou, T., McKeating, J. A., Bieniasz, P. D. & Rice, C. M. (2007). Claudin-1 is a hepatitis C virus co-receptor required for a late step in entry. *Nature* **446**, 801–805.

Goffard, A., Callens, N., Bartosch, B., Wychowski, C., Cosset, F. L., Montpellier, C. & Dubuisson, J. (2005). Role of N-linked glycans in the functions of hepatitis C virus envelope glycoproteins. *J Virol* **79**, 8400–8409.

Gottwein, J. M., Scheel, T. K., Hoegh, A. M., Lademann, J. B., Eugen-Olsen, J., Lisby, G. & Bukh, J. (2007). Robust hepatitis C genotype 3a cell culture releasing adapted intergenotypic 3a/2a (S52/JFH1) viruses. *Gastroenterology* **133**, 1614–1626.

Grakoui, A., McCourt, D. W., Wychowski, C., Feinstone, S. M. & Rice, C. M. (1993). A second hepatitis C virus-encoded proteinase. *Proc Natl Acad Sci U S A* **90**, 10583–10587.

Helle, F. & Dubuisson, J. (2008). Hepatitis C virus entry into host cells. *Cell Mol Life Sci* **65**, 100–112.

Hijikata, M., Mizushima, H., Akagi, T., Mori, S., Kakiuchi, N., Kato, N., Tanaka, T., Kimura, K. & Shimotohno, K. (1993a). Two distinct proteinase activities required for the processing of a putative nonstructural precursor protein of hepatitis C virus. *J Virol* **67**, 4665–4675.

Hijikata, M., Mizushima, H., Tanji, Y., Komoda, Y., Hirowatari, Y., Akagi, T., Kato, N., Kimura, K. & Shimotohno, K. (1993b). Proteolytic processing and membrane association of putative nonstructural proteins of hepatitis C virus. *Proc Natl Acad Sci U S A* **90**, 10773–10777.

Jones, C. T., Murray, C. L., Eastman, D. K., Tassello, J. & Rice, C. M. (2007). Hepatitis C virus p7 and NS2 proteins are essential for production of infectious virus. *J Virol* **81**, 8374–8383.

Kaul, A., Woerz, I., Meuleman, P., Leroux-Roels, G. & Bartenschlager, R. (2007). Cell culture adaptation of hepatitis C virus and *in vivo* viability of an adapted variant. *J Virol* **81**, 13168–13179.

Kuo, G., Choo, Q. L., Alter, H. J., Gitnick, G. L., Redeker, A. G., Purcell, R. H., Miyamura, T., Dienstag, J. L., Alter, M. J. & other authors (1989). An assay for circulating antibodies to a major etiologic virus of human non-A, non-B hepatitis. *Science* **244**, 362–364.

Lindenbach, B. D., Evans, M. J., Syder, A. J., Wolk, B., Tellinghuisen, T. L., Liu, C. C., Maruyama, T., Hynes, R. O., Burton, D. R. & other authors (2005). Complete replication of hepatitis C virus in cell culture. *Science* **309**, 623–626.

Lohmann, V., Korner, F., Koch, J., Herian, U., Theilmann, L. & Bartenschlager, R. (1999). Replication of subgenomic hepatitis C virus RNAs in a hepatoma cell line. *Science* **285**, 110–113.

Lohmann, V., Korner, F., Dobierzewska, A. & Bartenschlager, R. (2001). Mutations in hepatitis C virus RNAs conferring cell culture adaptation. *J Virol* **75**, 1437–1449.

Lorenz, I. C., Marcotrigiano, J., Dentzer, T. G. & Rice, C. M. (2006). Structure of the catalytic domain of the hepatitis C virus NS2–3 protease. *Nature* **442**, 831–835.

Manns, M. P., Foster, G. R., Rockstroh, J. K., Zeuzem, S., Zoulim, F. & Houghton, M. (2007). The way forward in HCV treatment – finding the right path. *Nat Rev Drug Discov* **6**, 991–1000.

Masaki, T., Suzuki, R., Murakami, K., Aizaki, H., Ishii, K., Murayama, A., Date, T., Matsuura, Y., Miyamura, T., Wakita, T. & Suzuki, T. (2008). Interaction of hepatitis C virus nonstructural protein 5A with core

protein is critical for the production of infectious virus particles. *J Virol* 82, 7964–7976.

McLauchlan, J., Lemberg, M. K., Hope, G. & Martoglio, B. (2002). Intramembrane proteolysis promotes trafficking of hepatitis C virus core protein to lipid droplets. *EMBO J* 21, 3980–3988.

Miyanari, Y., Atsuzawa, K., Usuda, N., Watashi, K., Hishiki, T., Zayas, M., Bartenschlager, R., Wakita, T., Hijikata, M. & Shimotohno, K. (2007). The lipid droplet is an important organelle for hepatitis C virus production. *Nat Cell Biol* 9, 1089–1097.

Muramatsu, S., Ishido, S., Fujita, T., Itoh, M. & Hotta, H. (1997). Nuclear localization of the NS3 protein of hepatitis C virus and factors affecting the localization. *J Virol* 71, 4954–4961.

Murray, C. L., Jones, C. T., Tassello, J. & Rice, C. M. (2007). Alanine scanning of the hepatitis C virus core protein reveals numerous residues essential for production of infectious virus. *J Virol* 81, 10220–10231.

Owsianka, A. M., Timms, J. M., Tarr, A. W., Brown, R. J., Hickling, T. P., Szwejk, A., Bienkowska-Szewczyk, K., Thomson, B. J., Patel, A. H. & Ball, J. K. (2006). Identification of conserved residues in the E2 envelope glycoprotein of the hepatitis C virus that are critical for CD81 binding. *J Virol* 80, 8695–8704.

Penin, F., Brass, V., Appel, N., Ramboarina, S., Montserret, R., Ficheux, D., Blum, H. E., Bartenschlager, R. & Moradpour, D. (2004). Structure and function of the membrane anchor domain of hepatitis C virus nonstructural protein 5A. *J Biol Chem* 279, 40835–40843.

Pietschmann, T., Lohmann, V., Kaul, A., Krieger, N., Rinck, G., Rutter, G., Strand, D. & Bartenschlager, R. (2002). Persistent and transient replication of full-length hepatitis C virus genomes in cell culture. *J Virol* 76, 4008–4021.

Pileri, P., Uematsu, Y., Campagnoli, S., Galli, G., Falugi, F., Petracca, R., Weiner, A. J., Houghton, M., Rosa, D. & other authors (1998). Binding of hepatitis C virus to CD81. *Science* 282, 938–941.

Poynard, T., Yuen, M. F., Ratziu, V. & Lai, C. L. (2003). Viral hepatitis C. *Lancet* 362, 2095–2100.

Roccasecca, R., Ansuini, H., Vitelli, A., Meola, A., Scarselli, E., Acali, S., Pezzanera, M., Ercole, B. B., McKeating, J. & other authors (2003). Binding of the hepatitis C virus E2 glycoprotein to CD81 is strain specific and is modulated by a complex interplay between hypervariable regions 1 and 2. *J Virol* 77, 1856–1867.

Russell, R. S., Meunier, J. C., Takikawa, S., Faulk, K., Engle, R. E., Bukh, J., Purcell, R. H. & Emerson, S. U. (2008). Advantages of a single-cycle production assay to study cell culture-adaptive mutations of hepatitis C virus. *Proc Natl Acad Sci U S A* 105, 4370–4375.

Saito, I., Miyamura, T., Ohbayashi, A., Harada, H., Katayama, T., Kikuchi, S., Watanabe, Y., Koi, S., Onji, M. & other authors (1990). Hepatitis C virus infection is associated with the development of hepatocellular carcinoma. *Proc Natl Acad Sci U S A* 87, 6547–6549.

Scarselli, E., Ansuini, H., Cerino, R., Roccasecca, R. M., Acali, S., Filocamo, G., Traboni, C., Nicosia, A., Cortese, R. & Vitelli, A. (2002). The human scavenger receptor class B type I is a novel candidate receptor for the hepatitis C virus. *EMBO J* 21, 5017–5025.

Schaller, T., Appel, N., Koutsoudakis, G., Kallis, S., Lohmann, V., Pietschmann, T. & Bartenschlager, R. (2007). Analysis of hepatitis C virus superinfection exclusion by using novel fluorochrome gene-tagged viral genomes. *J Virol* 81, 4591–4603.

Sumpter, R., Jr, Loo, Y. M., Foy, E., Li, K., Yoneyama, M., Fujita, T., Lemon, S. M. & Gale, M., Jr (2005). Regulating intracellular antiviral defense and permissiveness to hepatitis C virus RNA replication through a cellular RNA helicase, RIG-I. *J Virol* 79, 2689–2699.

Takigawa, Y., Nagano-Fujii, M., Deng, L., Hidajat, R., Tanaka, M., Mizuta, H. & Hotta, H. (2004). Suppression of hepatitis C virus replicon by RNA interference directed against the NS3 and NS5B regions of the viral genome. *Microbiol Immunol* 48, 591–598.

Tellinghuisen, T. L., Marcotrigiano, J., Gorbalenya, A. E. & Rice, C. M. (2004). The NS5A protein of hepatitis C virus is a zinc metalloprotein. *J Biol Chem* 279, 48576–48587.

Tellinghuisen, T. L., Marcotrigiano, J. & Rice, C. M. (2005). Structure of the zinc-binding domain of an essential component of the hepatitis C virus replicase. *Nature* 435, 374–379.

Tellinghuisen, T. L., Foss, K. L., Treadaway, J. C. & Rice, C. M. (2008). Identification of residues required for RNA replication in domains II and III of the hepatitis C virus NS5A protein. *J Virol* 82, 1073–1083.

Wakita, T., Pietschmann, T., Kato, T., Date, T., Miyamoto, M., Zhao, Z., Murthy, K., Habermann, A., Krausslich, H. G. & other authors (2005). Production of infectious hepatitis C virus in tissue culture from a cloned viral genome. *Nat Med* 11, 791–796.

Yamaga, A. K. & Ou, J. H. (2002). Membrane topology of the hepatitis C virus NS2 protein. *J Biol Chem* 277, 33228–33234.

Yi, M., Villanueva, R. A., Thomas, D. L., Wakita, T. & Lemon, S. M. (2006). Production of infectious genotype 1a hepatitis C virus (Hutchinson strain) in cultured human hepatoma cells. *Proc Natl Acad Sci U S A* 103, 2310–2315.

Yi, M., Ma, Y., Yates, J. & Lemon, S. M. (2007). Compensatory mutations in E1, p7, NS2, and NS3 enhance yields of cell culture-infectious intergenotypic chimeric hepatitis C virus. *J Virol* 81, 629–638.

Zhong, J., Gastaminza, P., Cheng, G., Kapadia, S., Kato, T., Burton, D. R., Wieland, S. F., Uprichard, S. L., Wakita, T. & Chisari, F. V. (2005). Robust hepatitis C virus infection *in vitro*. *Proc Natl Acad Sci U S A* 102, 9294–9299.

Zhong, J., Gastaminza, P., Chung, J., Stamataki, Z., Isogawa, M., Cheng, G., McKeating, J. A. & Chisari, F. V. (2006). Persistent hepatitis C virus infection *in vitro*: coevolution of virus and host. *J Virol* 80, 11082–11093.

JOURNAL OF VIROLOGY, May 2009, p. 5137–5147
0022-538X/09/$08.00+0 doi:10.1128/JVI.02179-08

Vol. 83, No. 10

Involvement of Creatine Kinase B in Hepatitis C Virus Genome Replication through Interaction with the Viral NS4A Protein▽

Hiromichi Hara,[1,2] Hideki Aizaki,[1] Mami Matsuda,[1] Fumiko Shinkai-Ouchi,[3] Yasushi Inoue,[1,4] Kyoko Murakami,[1] Ikuo Shoji,[1,5] Hayato Kawakami,[6] Yoshiharu Matsuura,[7] Michael M. C. Lai,[8] Tatsuo Miyamura,[1] Takaji Wakita,[1] and Tetsuro Suzuki[1]*

Department of Virology II[1] and Department of Biochemistry and Cell Biology,[3] National Institute of Infectious Diseases, Tokyo 162-8640, Japan; Department of Internal medicine, Division of Pulmonary Diseases, The Jikei University School of Medicine, Tokyo 105-8461, Japan[2]; Mita Hospital, International University of Health and Welfare, Tokyo 108-8329, Japan[4]; Division of Microbiology, Kobe University Graduate School of Medicine, Hyogo 650-0017, Japan[5]; Department of Anatomy, Kyorin University School of Medicine, Tokyo 181-8611, Japan[6]; Research Institute for Microbial Diseases, Osaka University, Osaka 565-0871, Japan[7]; and Department of Molecular Microbiology and Immunology, University of Southern California, Keck School of Medicine, Los Angeles, California 90033[8]

Received 15 October 2008/Accepted 20 February 2009

Persistent infection with hepatitis C virus (HCV) is a major cause of chronic liver diseases. The aim of this study was to identify host cell factor(s) participating in the HCV replication complex (RC) and to clarify the regulatory mechanisms of viral genome replication dependent on the host-derived factor(s) identified. By comparative proteome analysis of RC-rich membrane fractions and subsequent gene silencing mediated by RNA interference, we identified several candidates for RC components involved in HCV replication. We found that one of these candidates, creatine kinase B (CKB), a key ATP-generating enzyme that regulates ATP in subcellular compartments of nonmuscle cells, is important for efficient replication of the HCV genome and propagation of infectious virus. CKB interacts with HCV NS4A protein and forms a complex with NS3-4A, which possesses multiple enzyme activities. CKB upregulates both NS3-4A-mediated unwinding of RNA and DNA in vitro and replicase activity in permeabilized HCV replicating cells. Our results support a model in which recruitment of CKB to the HCV RC compartment, which has high and fluctuating energy demands, through its interaction with NS4A is important for efficient replication of the viral genome. The CKB-NS4A association is a potential target for the development of a new type of antiviral therapeutic strategy.

Hepatitis C virus (HCV) infection represents a significant global healthcare burden, and current estimates suggest that a minimum of 3% of the world's population is chronically infected (4, 19). The virus is responsible for many cases of severe chronic liver diseases, including cirrhosis and hepatocellular carcinoma (4, 16, 19). HCV is a positive-stranded RNA virus belonging to the family *Flaviviridae*. Its ~9.6-kb genome is translated into a single polypeptide of about 3,000 amino acids (aa), in which the nonstructural (NS) proteins NS2, NS3, NS4A, NS4B, NS5A, and NS5B reside in the C-terminal half region (6, 34, 44). NS4A, a small 7-kDa protein, functions as a cofactor for NS3 to enhance NS3 enzyme activities such as serine protease and helicase activities. The hydrophobic N-terminal region of NS4A, which is predicted to form a transmembrane α-helix, is responsible for membrane anchorage of the NS3-4A complex (8, 44, 50), and the central region of NS4A is important for the interaction with NS3 (10, 44). A recent study demonstrated the involvement of the C terminus of NS4A in the regulation of NS5A hyperphosphorylation and viral replication (28).

The development of HCV replicon technology several years ago accelerated research on viral RNA replication (7, 44). Furthermore, a robust cell culture system for propagation of infectious HCV particles was developed using a viral genome of HCV genotype 2a, JFH-1 strain, enabling us to study every process in the viral life cycle (27, 47, 54). RNA derived from genotype 1a, HCV H77, containing cell-culture adaptive mutations, also produces infectious viruses (52). Using these systems, it has been reported that the HCV genome replicates in a distinct, subcellular replication complex (RC) compartment, which includes NS3-5B and the viral RNA (2, 14, 33). The RC forms in a distinct compartment with high concentrations of viral and cellular components located on detergent-resistant membrane (DRM) structures, possibly a lipid-raft structure (2, 41), which may protect the RC from external proteases and nucleases. Almost all processes in viral replication are dependent on the host cell's machinery and involve intimate interaction between viral and host proteins. However, the functional roles of host factors interacting with the HCV RC in viral genome replication remain ambiguous.

To gain a better understanding of cellular factors that are components of the HCV RC and that function as regulators of viral replication, a comparative proteomic analysis of DRM fractions from HCV replicon and parental cells and subsequent RNA interference (RNAi) silencing of selected genes were performed. We identified creatine kinase B (CKB) as a key factor for the HCV genome replication. CKB catalyzes the reversible transfer of the phosphate group of phosphocreatine

* Corresponding author. Mailing address: Department of Virology II, National Institute of Infectious Diseases, 1-23-1 Toyama, Shinjuku-ku, Tokyo 162-8640, Japan. Phone: 81-3-5285-1111. Fax: 81-3-5285-1161. E-mail: tesuzuki@nih.go.jp.
▽ Published ahead of print on 4 March 2009.

(pCr) to ADP to yield ATP and creatine and is known to play important roles in local delivery and cellular compartmentalization of ATP (48, 51). The findings obtained here suggest that recruitment of CKB to the HCV RC, through CKB interaction with NS4A, is essential for maintenance or enhancement of viral replicase activity.

MATERIALS AND METHODS

Cell lines, antibodies, and reagents. Human hepatoma cell line Huh-7.5.1 (54) was kindly provided by Francis V. Chisari. Cell lines carrying subgenomic replicon RNAs, namely, SGR-N (41) and SGR-JFH1 (23), were derived from the HCV-N (17) and JFH-1 strains (24), respectively. Mouse monoclonal antibodies (MAbs) against HCV NS3 (Chemicon, Temecula, CA), NS4A (Santa Cruz Biotechnology, Inc., Santa Cruz, CA), NS5A (Biodesign, Saco, ME), NS5B (2), FLAG (M2; Sigma-Aldrich, St. Louis, MO), glyceraldehyde-3-phosphate dehydrogenase (GAPDH; Chemicon), and Flotillin-1 (BD Biosciences, San Jose, CA) and polyclonal antibodies (PAbs) against CKB (mouse [Abnova, Taipei, Taiwan], goat [Santa Cruz]), hemagglutinin (HA; Sigma-Aldrich), and FLAG (Sigma-Aldrich) were used. Cyclocreatine (Ccr; also known as 2-imino-1-imidazolidineacetic acid), pCr, and phosphopyruvic acid (pPy) were purchased from Sigma-Aldrich. Recombinant CKB and pyruvate kinase (PK) were obtained from Acris (Herfold, Germany) and Calbiochem (San Diego, CA), respectively.

Proteome analysis. RC-rich membrane fractions of cells were isolated as described previously (2, 41). Briefly, cells were lysed in hypotonic buffer. After removing the nuclei, supernatants were treated with 1% NP-40 for 60 min, mixed with 70% sucrose, overlaid with 55 and 10% sucrose, and centrifuged at 38,000 rpm for 14 h. Proteins from membrane fractions were purified by using a 2D Clean-Up kit (GE Healthcare, Tokyo, Japan), followed by labeling with fluorescent dyes: Cy5 for replicon cells, Cy3 for parental cells, and Cy2 for the protein standard containing equal amounts of both cell samples. Two-dimensional fluorescence difference gel electrophoresis (2D-DIGE) was performed using Immobiline DryStrip as the first-dimension gel and 12.5% polyacrylamide gel as the second-dimension gel. The 2D-DIGE images were analyzed quantitatively using the DeCyder software (GE Healthcare). Student *t* test was performed on differences between the tested samples using DeCyder biological variation analysis module. Samples were analyzed in triplicate. The protein spots of interest were excised from the gel, subjected to in-gel digestion using trypsin or lysyl endopeptidase and analyzed by liquid chromatography (MAGIC 2002 System; Michrom Bioresources, Auburn, CA) directly connected to electrospray ionization-ion trap mass spectrometry (LCQ-decaXP; Thermo Electron Corp., Iwakura, Japan). The results were subjected to database (NCBInr) search by Mascot server software (Matrix Science, Boston, MA) for peptide assignment.

Plasmids. A human CKB cDNA (43; kindly provided by Oriental Yeast Corp., Tokyo, Japan) was inserted into the EcoRI site of pCAGGS, yielding pCAGCKB. To generate expression plasmids for HA-tagged versions of wild-type and deletion mutated CKB, the corresponding DNA fragments were amplified by PCR, followed by introduction into the BglII site of pCAGGS. A fragment representing the inactive mutant CKB-C283S was synthesized by PCR mutagenesis. To generate FLAG-tagged NS protein expression plasmids, DNA fragments encoding either NS3, NS4A, NS4B, NS5A, or NS5B protein were amplified from HCV strains NIHJ1 (1) and JFH-1 (23) by PCR, followed by cloning into the EcoRI-EcoRV sites of pcDNA3-MEF (20). To generate an HA-tagged NS3 expression plasmid, a fragment encoding NS3 with the HA tag sequence at its N terminus was inserted into pCAGGS.

siRNA transfection. The small interfering RNAs (siRNAs) targeted to CKB (CKB-1 [5′-UAAGACCUUCCUGGUGUGGTT-3′] and CKB-2 [5′-CGUCAC CCUUGGUAGAGUUTT-3′]) and the scramble negative control siRNA to CKB-2 (5′-GGCGUACUAGCUUAUUCGCTT-3′) were purchased from Sigma. Cells in a 24-well plate were transfected with siRNA using HiPerFect transfection reagent (Qiagen, Tokyo, Japan) according to the manufacturer's instructions. The siRNA sequences for the other genes used in the siRNA screening are available upon request.

HCV infection. Culture media from Huh-7 cells transfected with in vitro-transcribed RNA corresponding to the full-length JFH-1 (47) was collected, concentrated, and used for the infection assay (3).

Quantification of HCV core protein and RNA. To estimate the levels of HCV core protein, aliquots of culture supernatants or of cell lysates were assayed by using HCV Core enzyme-linked immunosorbent assay kits (5). Total RNA was isolated from harvested cells using TRIzol (Invitrogen, Carlsbad, CA). Copy numbers of the viral RNA were determined by reverse transcription-PCR (RT-PCR) (2, 36, 46).

Immunoprecipitation, immunoblot analysis, and immunofluorescence microscopy. The analyses, as well as DNA transfection, were performed essentially as previously described (42). Cells were lysed in immunoprecipitation lysis buffer (50 mM Tris-HCl [pH 7.6], 150 mM NaCl, 1% sodium deoxycholate, 1% NP-40, 0.1% sodium dodecyl sulfate, 1 mM dithiothreitol, 1 mM calcium acetate). For immunoprecipitation, supernatants of cell lysates were precipitated with anti-FLAG antibody and protein A-Sepharose Fast Flow beads (GE healthcare). For immunofluorescence microscopy, anti-CKB goat PAb and anti-NS4A MAb as primary antibodies and Alexa Fluor 555-conjugated donkey anti-goat immunoglobulin G (Invitrogen) and Alexa Fluor 488-conjugated rabbit anti-mouse immunoglobulin G (Invitrogen) as secondary antibodies were used and observed under an LSM 510 confocal microscope (Carl Zeiss, Oberkochen, Germany).

Immunoelectron microscopy. Postembedding immunostaining using the colloidal gold-labeling method was performed as described previously (38). Cells were fixed in 4% paraformaldehyde–1% glutaraldehyde at 4°C for 1 h. After dehydration through a graded series of ethanol, cells were embedded in LR White (London Resin Company, London, United Kingdom) and sectioned. After blocking, section grids were incubated with a mixture of anti-NS4A and anti-CKB antibodies at 4°C overnight, followed by treatment with a mixture of 18-nm colloidal gold-conjugated donkey anti-mouse immunoglobulin G and 12-nm colloidal gold-conjugated donkey anti-goat immunoglobulin G antibodies (Jackson Immunoresearch, West Grove, PA) at 4°C overnight. The sections were stained with uranyl acetate and observed under a transmission electron microscope.

Measurement of CK activity and cellular ATP level. Cells were lysed with passive lysis buffer (Promega, Madison, WI), and CK activities were measured based on Oliver methods (40), in which the activity of converting creatine phosphate and ADP to creatine and ATP was measured. ATP levels in cell lysates were measured by using a CellTiter-Glo luminescent cell viability assay (Promega).

RNA replication assays in permeabilized replicon cells and in vitro. The RNA synthesis assay using permeabilized replicon cells was based on a previously described method (33). Briefly, SGR-JFH1 cells were treated with 5 μg of actinomycin D/ml for 2 h, followed by permeabilization with 50 μg of digitonin/ml for 5 min. The resulting mix was incubated with 500 μM concentrations of ATP, GTP, and CTP; 10 μCi of UTP ([α-^{32}P]UTP); 50 μg of actinomycin D/ml; and 5 mM pCr with or without 20 U of CKB/ml for 4 h at 27°C. RNA was extracted by using TRIzol and analyzed by 1% formaldehyde agarose gel electrophoresis. The cell-free RNA replication assay was performed as described previously (2).

In vitro helicase assays. Helicase activity on double-stranded RNA (dsRNA) was investigated as described previously (11) with some modifications. The 5′ end of the release strand was labeled with [γ-^{32}P]ATP using T4 polynucleotide kinase (Ambion). The dsRNA substrate was obtained by annealing the labeled RNA with a template strand RNA at a molar ratio of 1:1. The helicase assay mixture contained 5 nM dsRNA, helicase enzyme (80 nM NS3 or NS3-4A [kindly provided by R. De Francesco]), 6 mM ATP, in the presence or absence of 20 U of CKB/ml in an assay buffer (25 mM MOPS-NaOH [pH 7.0], 2.5 mM dithiothreitol, 100 μg of bovine serum albumin/ml, 3 mM $MgCl_2$, 5 mM pCr, 2.5 U of RNase inhibitor/ml). After the helicase reaction, samples were electrophoresed in a native 8% polyacrylamide gel and autoradiographed.

To determine the effect of PK/pPy system on the helicase activity, PK and pPy were used instead of CKB and pCr. Helicase activity on dsDNA was measured based on homogeneous time-resolved fluorescence quenching using a Trupoint helicase assay kit (Perkin-Elmer, Waltham, MA) according to the manufacturer's instructions.

In vitro protease assay. In vitro HCV protease activity of NS3-4A or NS3 was analyzed by using a SensoLyteHCV protease assay kit (AnaSpec, San Jose, CA) according to the manufacturer's instructions.

RESULTS

Identification of host factors involved in HCV RNA replication by comparative proteomic analysis of DRM fractions and RNAi silencing. To identify host proteins involved in the HCV RC, proteome profiles of the RC-rich membrane fraction in Huh-7 cells harboring subgenomic replicon RNA derived from genotype 1b, N isolate (SGR-N) were compared to those of parental cells by 2D-DIGE. We confirmed that the DRM fraction obtained from SGR-N cells is functionally active in a

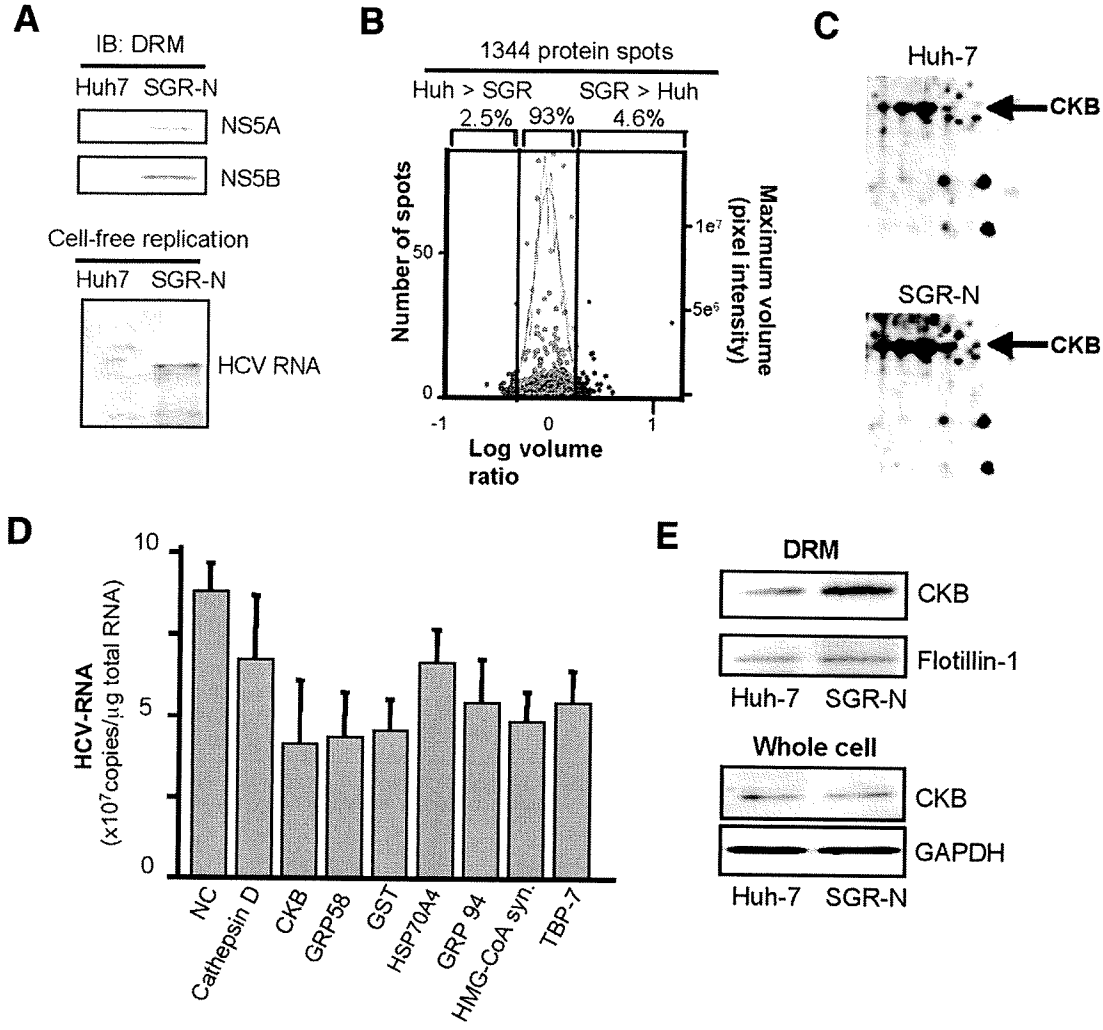

FIG. 1. Comparative proteomic analysis of DRM fractions and RNAi silencing. (A) Preparation of functionally active RC fraction for proteome analysis. DRM fractions obtained from SGR-N cells and parental Huh-7 cells were analyzed by immunoblotting with anti-NS5A and anti-NS5B antibodies (upper panel) and by the cell-free RNA replication assay (lower panel). (B) Histogram representation of proteins detected in 2D-DIGE. Images were analyzed quantitatively by the DeCyder software. The left and right *y* axis, respectively, indicate the spot frequency and the maximum volume of each spot, given against the log volume ratio (*x* axis). (C) Comparison of 2D-DIGE maps of proteins from DRM fractions of SGR-N cells and Huh-7 cells. Enlarged 2D-DIGE gel images of regions containing protein spots of CKB (arrows) are shown. (D) Effects of siRNAs of genes selected from comparative proteome analysis on HCV RNA replication. SGR-N cells were transfected with siRNA specific to cathepsin D, CKB (siCKB-1), GRP58, GST, Hsp70 protein 4, GRP94, HMG-coenzyme A synthase, or Tat binding protein 7 or with nontargeting (NC) siRNA. At 48 h posttransfection, total RNA was isolated and HCV RNA levels were assessed by real-time RT-PCR. (E) Enrichment of CKB in the DRM of HCV replicon cells. Equal amounts of DRM fractions from SGR-N and parental Huh-7 cells, or whole-cell lysates from both cells were analyzed by immunoblotting with antibodies against CKB, flotilin-1 or GAPDH.

cell-free replication assay (Fig. 1A). Three independent proteome experiments were performed for a reliable analysis of protein expression. Approximately 1,300 spots were resolved in each gel, and 4 to 5% of the protein spots represented a >2-fold increase in the membrane fraction of replicon cells in each experiment (Fig. 1B). The protein spots that exhibited high reproducibility (an example shown in Fig. 1C) were excised, digested by trypsin or lysyl endopeptidase, and analyzed by mass spectrometry, which identified the corresponding proteins in 27 cases (Table 1). Among the proteins implicated in a variety of functional categories, 10 were involved in protein folding, mainly as chaperones, 7 were metabolic and biosynthesis enzymes including proteins for redox regulation or energy pathways, 3 were involved in cytoskeleton organization, and 3 proteins were related to cellular processes, mainly proteolysis pathways. The viral NS proteins identified as differentially expressed proteins in the analysis were not listed.

In order to identify host factors involved in HCV replication, we examined the effects on viral RNA replication of transfection of SGR-N cells with siRNAs against genes encoding nine proteins belonging to diverse classes of biological functions (Table 1). Each siRNA reduced the HCV RNA level to 47 to 76% of the level of the siRNA control (Fig. 1D). None of the siRNAs tested exhibited considerable cytotoxicity against the replicon cells, ruling out overt toxicity as a mechanism for inhibition of viral RNA replication. Among the candidate

TABLE 1. Selected proteins that reproducibly increased in the DRM fraction of SGR-N cells[a]

Avg ratio	*P* (Student *t* test)	Coverage (%)	Protein name	Molecular function	GI no.
5.56	0.04	27	GRP94	Protein folding	15010550
4.99	0.07	47	Hsp60	Protein folding	6996447
3.73	0.07	6	tRNA guanine transglycosylase	Metabolism	30583205
3.56	0.06	23	KIAA0088	Unknown	577295
3.32	0.07	4	Thioredoxin-related protein	Unknown	20067392
3.32	0.13	12	Tat binding protein 1 (TBP-1)	Cellular processes	20532406
3.06	0.14	22	Aldehyde dehydrogenase 1	Metabolism	2183299
3.06	0.14	14	Chaperonin TRiC/CCT, subunit 2	Protein folding	54696794
2.96	0.04	14	Heat shock 70-kDa protein 4 (HSPA4)	Protein folding	6226869
2.96	0.04	29	GRP58	Metabolism/protein folding	2245365
2.94	0.01	37	Mutant β-actin	Cytoskeleton organization	28336
2.65	0.17	33	Glutathione S-transferase (GST)	Catalytic activity	2204207
2.53	0.04	37	Keratin 19	Cytoskeleton organization	6729681
2.46	0.08	6	Heterogeneous nuclear ribonucleoprotein K	Nucleic acid modification	460789
2.45	0.001	13	HMG-coenzyme A synthase	Metabolism	30009
2.4	0.02	31	CKB	Energy pathway/metabolism	180570
2.4	0.02	11	Cathepsin D	Cellular processes	30582659
2.4	0.02	11	C8orf2	Unknown	37181322
2.36	0.1	38	Tropomyosin 4-anaplastic lymphoma kinase fusion protein	Cytoskeleton organization	14010354
2.36	0.1	6	Calreticulin	Protein folding	30583735
2.33	0.01	29	Quinolinate phosphoribosyltransferase	Metabolism	30583301
2.29	0.04	25	Protein disulfide isomerase-related protein 5	Protein folding	1710248
2.29	0.04	16	Tat binding protein 7 (TBP-7)	Cellular processes	263099
2.05	0.11	24	Calumenin	Metabolism	2809324
2.05	0.12	10	TRiC/CCT, subunit 5	Protein folding	24307939
2.03	0.07	20	Hsp90 beta	Protein folding	34304590
2.01	0.07	10	TRiC/CCT, subunit 1	Protein folding	36796

[a] The spectra obtained by tandem mass spectrometry were collected using data-dependent mode, and the results were subjected to database (NCBInr) search by Mascot server software (Matrix Science, London, United Kingdom) for peptide assignment. Coverage, the ratio of the portion of protein sequence covered by matched peptides to the whole protein sequence. GI no., GenInfo identifier number.

genes examined, we observed a reproducible inhibition of HCV RNA replication by two independent siRNAs targeting CKB (see below).

CKB participates in HCV RNA replication and the propagation of infectious virus. CKB is a brain-type creatine kinase isoenzyme and is also detected in a variety of other tissues, including human liver (32). Steady-state levels of CKB in the DRM fraction, as well as in whole-cell lysate of SGR-N cells were compared to those from parental cells by Western blotting. The CKB level in the DRM fraction of replicon cells was higher than that in parental cells (Fig. 1E), confirming the results of the proteome analysis described above. In contrast, the CKB level in whole cells was similar in both cells (Fig. 1E). These results suggest participation of posttranslational modification, such as translocation to the DRM fraction, of CKB in replicon cells.

Figure 2A shows the inhibitory effect on HCV RNA replication of CKB siRNA; siCKB-2, the sequence of which does not overlap with the sequence of siCKB-1 used in the above siRNA screening (Fig. 1D). Transfection with siCKB-2 effectively decreased the cellular level of CKB enzymatic activity (data not shown), as well as the abundance of CKB protein (Fig. 2A), and resulted in 60% reduction in the viral RNA level in SGR-N cells compared to the cells treated with control siRNA. This inhibitory effect of siRNA on HCV RNA abundance was also observed in JFH-1-derived subgenomic replicon (SGR-JFH1) cells. The viral RNA level in the cells transfected with siCKB-2 decreased by 50% compared to the control (Fig. 2A). We also tested the CKB mutant, CKB-C283S, in which Cys at aa 283, near the catalytic site, has been replaced with Ser (Fig. 3A) and which is known to be enzymatically inactive and to work in a dominant-negative manner (22, 29). As expected, overexpression of CKB-C283S resulted in a reduction in HCV RNA replication in SGR-N cells (Fig. 2B). We obtained a similar result in SGR-JFH1 cells, as described below (Fig. 3E).

To further examine the involvement of CKB in HCV RNA replication, we tested the effect of Ccr, a substrate analogue and possible inhibitor for CK in either SGR-N, SGR-JFH1 (Fig. 2C), or Huh7 cells transiently replicating luciferase-subgenomic replicon (data not shown). We found dose-dependent inhibition of HCV RNA replication but no observed effect on total cellular levels of protein and ATP (Fig. 2D) in the replicon setting used.

We next examined whether the knockdown of CKB or treatment with Ccr would abrogate the production of HCVcc. At 72 h posttransfection with siCKB-2, the HCV core level in cells infected with HCVcc was significantly reduced (Fig. 2E). Treatment of the infected cells with Ccr at various concentrations also reduced the intracellular and supernatant core level and subsequently decreased HCVcc production (Fig. 2F). These results demonstrate that suppression of the HCV RNA replication by the siRNA-mediated knockdown of CKB or treatment with CKB inhibitor leads to reduction of the production of infectious virus.

CKB interacts with HCV NS4A. Having established a role for CKB in HCV RNA replication, we then tried to determine to how CKB influences the HCV life cycle. It has been re-